Table II. Complications after pancreaticoduodenectomy

Parameter	*Nonwrapping group* (n = *1,679*)	*Wrapping group* (n = *918*)*	P *value*
Pancreatic fistula			
All grades	627 (37.3)	393 (42.8)	.006
Grade B + C	281 (16.7)	198 (21.6)	.002
Delayed gastric empting	182 (10.8)	117 (12.7)	.146
Bile leakage	52 (3.1)	29 (3.2)	.931
Intra-abdominal abscess	179 (10.7)	111 (12.1)	.269
Intra-abdominal hemorrhage†			
Early	32 (1.9)	14 (1.5)	.482
Late	22 (1.3)	18 (2.0)	.198
Wound infection	151 (9.0)	115 (12.5)	.005
Other organ complications			
Respiratory	76 (4.6)	43 (4.7)	.859
Cardiac	25 (1.5)	28 (3.1)	.007
Vascular	24 (1.4)	20 (2.2)	.157
Renal	17 (1.0)	4 (0.4)	.117
Mortality	22 (1.3)	9 (1.0)	.459
Postoperative hospital stay, days (mean ± SD)	38.0 ± 37.9	41.3 ± 30.1	.014

*Wrapping of pancreatic anastomosis or vessels, including hepatic artery, using omentum or falciform ligament.
†Early intra-abdominal hemorrhage indicates incomplete hemostasis and a failure of carrying out sufficient intraoperative management. It was defined as occurring within 3 days after pancreaticoduodenectomy, and it was not associated with any other postoperative complications. Late intra-abdominal hemorrhage is associated with other postoperative complications, including pancreatic fistula and intra-abdominal abscess.

Table III. Postoperative drainage after pancreaticoduodenectomy

		*Wrapping group**	
Parameter	*Nonwrapping group* (n = *1,679*)	*Falciform ligament* (n = *219*)	*Omentum* (n = *699*)
Amylase level of postoperative drainage fluid (IU/l)			
POD1	4,405 ± 14,129	4,802 ± 17,644	4,950 ± 13,324
POD3	2,924 ± 2,963	2,077 ± 10,947	1,317 ± 2,963†
POD4	1,384 ± 6,876	327 ± 639	1,395 ± 8,227

*Wrapping of pancreatic anastomosis or vessels, including hepatic artery, using omentum or falciform ligament.
†$P = .027$ (nonwrapping versus omentum).
POD, Postoperative day.

DISCUSSION

This study was a report with a large number of patients on the effect of omentum wrapping or falciform ligament after a PD by a retrospective analysis after the report of ISGPF definition.[16] Each institution had their own criteria for pancreatic fistula before the publication of the definition of pancreatic fistula by an ISGPF. Therefore, it was difficult to compare the incidence of pancreatic fistula. The members of the JSPS now share the same definition of pancreatic fistula, and we can accumulate clinical data to compare the incidence of pancreatic fistula by using this common definition. These data were collected between January 2006 and June 2008. However, only 65% of the institutions could respond to the survey, because 35% of the institutions do not have database systems that can evaluate the incidence of pancreatic fistula according to the ISGPF criteria. Seven independent risk factors were identified for grade B + C pancreatic fistula, 4 factors for early intra-abdominal hemorrhage, and 2 factors for late intra-abdominal hemorrhage. Although the evaluation of delayed gastric emptying and intra-abdominal hemorrhage should be based on grading of ISGPS,[21,22] this study was conducted as a retrospective study, and it was difficult to accumulate sufficient data based on the ISGPS criteria that were reported in 2007.

The incidence of pancreatic fistula was significantly higher in the wrapping group in comparison to the nonwrapping group; moreover, the incidence of grade B + C pancreatic fistula was also higher in the wrapping group. However, the amylase level of the drainage fluid was lower in

Table IV. Complications according to the material used by wrapping

Parameter	*Nonwrapping group* (n = *1,679*)	*Wrapping group**			
		Falciform ligament, (%) (n = *219*)	P *value*†	*Omentum, (%)* (n = *699*)	P *value*†
Pancreatic fistula					
All grades	627 (37.3)	72 (32.8)	.197	321 (45.9)	<.001
Grade B + C	281 (16.7)	31 (14.2)	.332	167 (23.9)	<.001
Delayed gastric empting	182 (10.8)	25 (11.4)	.797	92 (13.2)	.106
Bile leakage	52 (3.1)	6 (2.7)	.773	23 (3.3)	.806
Intra-abdominal abscess	179 (10.7)	33 (15.1)	.051	78 (11.2)	.722
Intra-abdominal hemorrhage					
Early	32 (1.9)	3 (1.4)	.791	11 (1.6)	.580
Late	22 (1.3)	4 (0.5)	.532	14 (2.0)	.208
Wound infection	151 (9.0)	26 (11.8)	.168	89 (12.7)	.006
Other organ complications					
Respiratory	76 (4.6)	8 (3.7)	.554	35 (5.0)	.613
Cardiac	25 (1.5)	5 (2.3)	.382	23 (3.3)	.004
Vascular	24 (1.4)	8 (3.7)	.025	12 (1.7)	.601
Renal	17 (1.0)	1 (0.5)	.712	3 (0.4)	.156
Mortality	22 (1.3)	2 (0.9)	>.999	7 (1.0)	.532

*Wrapping of pancreatic anastomosis or vessels, including hepatic artery, using omentum or falciform ligament.
†Versus nonwrapping group.

Table V. Complications according to the location of wrapping

Parameter	*Nonwrapping group, (%)* (n = *1,679*)	*Wrapping group**			
		Vessels, (%) (n = *552*)	P *value*†	*Anastomosis,*‡ *(%)* (n = *366*)	P *value*†
Pancreatic fistula					
All grades	627 (37.3)	223 (40.4)	.200	170 (46.4)	.001
Grade B + C	281 (16.7)	110 (19.9)	.087	88 (24.0)	.001
Delayed gastric empting	182 (10.8)	52 (11.2)	.798	55 (15.1)	.023
Bile leakage	52 (3.1)	18 (3.3)	.848	11 (3.0)	.927
Intra-abdominal abscess	179 (10.7)	55 (9.9)	.643	56 (15.3)	.012
Intra-abdominal hemorrhage					
Early	32 (1.9)	4 (0.7)	.056	10 (2.7)	.313
Late	22 (1.3)	8 (1.4)	.806	10 (2.7)	.047
Wound infection	151 (9.0)	61 (11.1)	.153	54 (14.8)	.001
Other organ complications					
Respiratory	76 (4.6)	22 (4.0)	.591	21 (5.7)	.323
Cardiac	25 (1.5)	12 (2.2)	.274	16 (4.4)	<.001
Vascular	24 (1.4)	10 (1.8)	.525	10 (2.7)	.077
Renal	17 (1.0)	1 (0.2)	.059	3 (0.3)	.734
Mortality	22 (1.3)	6 (1.1)	.683	3 (0.8)	.602

*Wrapping of vessels, including hepatic artery, using omentum or falciform ligament.
†Versus nonwrapping group.
‡Pancreaticojejunostomy or pancreaticogastrostomy using either the omentum or falciform ligament.

patients with omental wrapping than that with other procedures. It might be suggested that the omental wrapping would disturb the drainage of oozing pancreatic juice, and that this may cause damage of the omentum. Indeed, omental wrapping is associated with complications, such as intestinal obstruction, necrosis of the omentum, and infection.[20]

A soft pancreas is susceptible to postoperative intra-abdominal hemorrhage, and a late intra-abdominal hemorrhage is a lethal complication. Omentum wrapping influenced the occurrence of intra-abdominal hemorrhage, which might be related to omentum wrapping, which is performed to protect skeletonized vessels when the surgeon considers the vessels to be fragile during an operation.

Table VI. Univariable analysis for pancreatic fistula

Parameter	*Pancreatic fistula**		P *value*
	With (n = *479*)	*Without* (n = *2,118*)	
Age, y (≥70/<70)	221/258	862/1,256	.029
Gender (male/female)	321/158	1,238/880	.010
Albumin, g/dL (≥3.5/<3.5)	354/108	1,674/383	.020
AST, IU/L (>40/<40)	211/257	807/1,261	.016
ALT, IU/L (>40/<40)	253/215	987/1,083	.013
Amylase, IU/L (>180/<180)	52/406	307/1,709	.034
Preoperative biliary drainage (yes/no)	248/231	973/1,145	.021
Pylorus preservation (yes/no)	282/197	1,118/1,000	.018
Extended resection (yes/no)	384/86	1,788/287	.013
Operation time, min (>600/<600)	116/354	378/1,693	.001
Blood loss, mL (>1,500/<1,500)	119/359	470/1,632	.233
Pancreatic texture (hard/soft)	389/90	1,070/1,048	<.001
Anastomosis (P-J/P-G)	439/40	1,876/242	.051
Duct-to-mucosal anastomosis (yes/no)	372/107	1,675/443	.491
Pancreatic stent (yes/no)	402/77	1,639/479	.002
Wrapping			<.001
Falciform ligament at pancreaticoenterostomy	5	3	
Falciform ligament at vessels	67	144	
Omentum at pancreaticoenterostomy	165	193	
Omentum at vessels	156	185	
No	627	1,052	

*Grade B + C pancreatic fistula according to the International Study Group of Pancreatic Fistula.
ALT, Alanine aminotransferase; *AST,* aspartate aminotransferase; *P-G,* pancreaticogastrostomy; *P-J,* pancreaticojejunostomy.

Table VII. Univariable analysis for intra-abdominal hemorrhage

Parameter	*Early intra-abdominal hemorrhage*			*Late intra-abdominal hemorrhage*		
	With (n = *46*)	*Without* (n = *2,551*)	P *value*	*With* (n = *40*)	*Without* (n = *2,557*)	P *value*
Age, y (≥70/<70)	25/21	1,058/1,493	.079	16/24	1,067/1,490	.826
Gender (male/female)	35/11	1,534/1,027	.025	32/8	1,527/1,030	.009
Albumin, g/dL (≥3.5/<3.5)	35/10	1,993/481	.641	29/11	1,999/480	.197
AST, IU/L (>40/<40)	20/26	998/1,492	.641	13/26	1,005/1,492	.382
ALT, IU/L (>40/<40)	25/21	1,215/1,277	.452	17/22	1,223/1,276	.507
Extended resection (yes/no)	35/10	2,137/363	.148	34/5	2,138/368	.744
Operation time, min (>600/<600)	18/30	478/2,017	.008	13/27	481/2,020	.035
Blood loss, mL (>1,500/<1,500)	15/31	574/1,960	.111	13/27	576/1,964	.142
Blood transfusion (yes/no)	27/18	776/1,642	<.001	9/27	794/1,633	.327
Pancreatic texture (hard/soft)	38/8	1,421/1,130	<.001	34/6	1,425/1,132	<.001
Anastomosis (P-J/P-G)	40/6	2,275/276	.630	35/5	2,280/277	.616
Duct-to-mucosal anastomosis (yes/no)	34/12	2,013/538	.411	31/9	2,016/541	.837
Pancreatic stent (yes/no)	38/8	2,003/548	.503	38/2	2,003/554	.011
Wrapping (yes/no)	14/32	904/1,647	<.001	22/18	1,657/900	.198
Omentum	11	688	.901	14	685	.562
At panceaticoenteric anastomosis	10	356	.109	10	356	.209

ALT, Alanine aminotransferase; *AST,* aspartate aminotransferase; *P-G,* pancreaticogastrostomy; *P-J,* pancreaticojejunostomy.

Surgeons might therefore have chosen to use wrapping for inappropriate cases or when they suspected an increased likelihood of leakage. If surgeons choose to use wrapping in worst cases, a high incidence of pancreatic fistula should be indicated in both omental wrapping and falciform ligament groups.

This study has revealed that wrapping using the omentum did not decrease the incidence of pancreatic fistula. However, this study has several

Table VIII. Risk factors for postoperative pancreatic fistula after pancreaticoduodenectomy according to a multivariable analysis

Predictor	P *value*	*Odds ratio (95% CI)*
Gender (male)	<.001	1.508 (1.200–1.896)
Albumin (<3.5 g/dL)	.035	1.332 (1.021–1.738)
Pancreas texture (soft)	<.001	4.129 (3.139–5.339)
Operation time (≥600 minutes)	.031	1.345 (1.027–1.761)
Extended resection	.013	1.461 (1.084–1.969)
Pylorus preservation	.032	1.276 (1.021–1.595)
Wrapping		
Omentum at pancreaticoenterostomy	.040	1.378 (1.104–1.871)
Omentum at vessels	.005	1.555 (1.141–2.120)

CI, Confidence interval.

limitations because it was a multicenter study using retrospective data collection, which makes it a potential source for significant bias. This study indicated that the usage of an omental flap does not reduce the occurrence of complications after PD, including the incidence of pancreatic fistula. A further validation study is therefore necessary to evaluate the efficacy of wrapping for PD.

The authors are especially grateful to the 91 leading Japanese institutions that kindly took part in the survey. These institutions are listed here:

Aichi Medical University, Department of Surgery; Division of Gastroenterological Surgery
Akita City Hospital, Department of Surgery
Asahikawa Medical College, Department of Gastroenterological Surgery
Chiba Cancer Center, Department of Gastroenterological Surgery
Chiba Rosai Hospital, Department of Surgery
Dokkyo Medical University, Department of Surgery II
Fujita Health University School of Medicine, Department of Biliary Pancreatic Surgery
Fukuoka University Faculty of Medicine, Department of Surgery
Fukui Red Cross Hospital, Department of Surgery
Fukui Saiseikai Hospital, Department of Surgery
Hachioji-Shokaki Hospital, Department of Surgery
Hamamatsu University School of Medicine, Department of Surgery II
Hino Municipal Hospital, Department of Surgery
Hirosaki University School of Medicine, Department of Surgery II
Hiroshima City Hospital, Department of Surgery
Hiroshima University Graduate School of Biomedical Sciences, Department of Surgery, Division of Clinical Medical Science
Hiroshima University Graduate School of Biomedical Sciences, Department of Surgery, Division of Frontier Medical Science
Hokkaido University Graduate School of Medicine, Department of General Surgery
Hyogo College of Medicine, Department of Surgery 1
Ise Municipal General Hospital, Department of Surgery
Itabashi Chuo Medical Center, Department of Surgery
Iwate Medical University School of Medicine, Department of Surgery
Jichi Medical University, Department of Surgery
Jikei University School of Medicine, Department of Surgery
Jikei University School of Medicine, Aoto Hospital, Department of Surgery
Jikei University, Daisan Hospital, Department of Surgery
Jikei University, Kashiwa Hospital, Department of Surgery
Kagawa University, Faculty of Medicine, Department of Gastroenterological Surgery
Kagoshima Medical Association Hospital, Department of Surgery
Kagoshima University, Department of Surgical Oncology
Kanazawa Medical University Hospital, Department of surgical Oncology
Kanazawa University Graduate School of Medical Science, Department of Gastroenterological Surgery
Keio University School of Medicine, Department of Surgery
Kitakyushu Municipal Medical Center, Department of Surgery
Kitasato University School of Medicine, Department of Surgery
Kobe University Graduate School of Medicine, Department of Hepato-Biliary-Pancreatic Surgery
Kumamoto University, Department of Gastroenterological Surgery
Kurume University School of Medicine, Department of Surgery

Kyorin University School of Medicine, Department of Surgery
Kyoto University, Department of Hepato-Biliary-Pancreatic Surgery and Transplantation
Kyushu University, Faculty of Medicine, Department of Surgery I
Matsunami General Hospital, Department of Surgery
Meiwa Hospital, Department of Surgery
Mie University Graduate School of Medicine, Department of Hepatobiliary Pancreatic Surgery
Miyagi Cancer Center, Department of Surgery
Miyazaki University School of Medicine, Department of Surgical Oncology and Regulation of Organ Function
Nagasaki Medical Center, Department of Surgery
Nagasaki University Graduate School of Medicine, Department of Gastroenterological Surgery
Nagasaki University Graduate School of Medicine, Department of Translational Medical Science
Nagoya City University Graduate School of Medical Sciences, Department of Gastroenterological Surgery
Nagoya University Graduate School of Medicine, Department of Gastroenterological Surgery
Nara Medical University, Department of Surgery
National Cancer Center Hospital East, Department of Upper Abdominal Surgery
Nihon University School of Medicine, Division of Digestive Surgery
Niigata Prefectural Central Hospital, Department of Surgery
Niigata University School of Medicine, Department of Surgery
Nippon Medical School, Department of Surgery I
Ogaki Municipal Hopital, Department of Surgery
Okayama University Medical School, Department of Surgery
Osaka City University Graduate School of Medicine, Department of Hepato-Biliary-Pancreatic Surgery
Osaka City University Graduate School of Medicine, Department of Surgical Oncology
Osaka Medical Center for Cancer and Cardiovascular Diseases, Department of Surgery
Osaka University Graduate School of Medicine, Department of Gastroentelogical Surgery
Rinku Medical Center, Department of Surgery
Saku Central Hospital, Department of Surgery
Saga University Faculty of Medicine, Department of Surgery
Sapporo Medical University, Department of Surgery I
Saitama Medical University International Medical Center, Department of Surgery
Shiga University of Medical Science, Department of Surgery
Shinshu University School of Medicine, Department of Surgery
Showa University School of Medicine, Department of Surgery
St. Marianna University School of Medicine, Department of Surgery
St. Marianna University, Yokohama City Seibu Hospital, Department of Surgery
Teikyo University, Department of Surgery
Teikyo University Chiba Medical Center, Department of Surgery
Tochigi Cancer Center, Department of Surgery
Tobata Kyoritsu Hospital, Department of Surgery
Tohoku University Graduate School of Medicine, Department of Surgery, Division of Hepato-Biliary-Pancreatic Surgery
Tokai University, School of Medicine, Department of Gastroenterological Surgery
Tokyo Medical and Dental University, Department of Hepato-Biliary-Pancreatic Surgery
Tokyo Medical and Dental University Ichikawa General Hospital, Department of Surgery
Tokyo Medical University, Department of Surgery
Tokyo Women's Medical University Medical Center East, Department of Surgery
Tokyo Women's Medical University, Institute of Gastroenterology, Department of Gastroenterological Surgery
University of Occupational and Environmental Health, Department of Surgery I
University of Yamanashi Faculty of Medicine, Department of Surgery I
Wakayama Medical University, Second Department of Surgery
Yamagata University Faculty of Medicine, Department of Gastroenterological and General Surgery
Yamaguchi University Graduate School of Medicine, Department of Digestive Surgery and Surgical Oncology
Yame General Hospital, Department of Surgery
Yokohama City University, Department of Gastroenterological Surgery.

REFERENCES

1. Yeo CJ, Cameron JL, Sohn TA, Lillemoe KD, Pitt HA, Talamini MA, et al. Six hundred fifty consecutive pancreaticoduodenectomies in the 1990s: pathology, complications, and outcomes. Ann Surg 1997;226:248-57.
2. Neoptolemos JP, Russell RCG, Bramhall S, Theis B. Low mortality following resection for pancreatic and periampullary tumours in 1026 patients: UK survey of specialist pancreatic units. Br J Surg 1997;84:1370-6.
3. Büchler MW, Friess H, Wagner M, Kulli C, Wagener V, Z'Graggen K. Pancreatic fistula after pancreatic head resection. Br J Surg 2000;87:883-9.

4. Winter JM, Cameron JL, Campbell KA, Arnold MA, Chang DC, Coleman J, et al. 1423 pancreaticoduodenectomies for pancreatic cancer: a single-institution experience. J Gastrointest Surg 2006;10:1199-211.
5. McPhee JT, Hill JS, Whalen GF, Zayaruzny M, Litwin DE, Sullivan ME, et al. Perioperative mortality for pancreatectomy: a national perspective. Ann Surg 2007;246: 246-53.
6. Moriura S, Ikeda S, Ikezawa T, Naiki K. The inclusion of an omental flap in pancreatoduodenectomy. Surg Today 1994; 24:940-1.
7. Fong Y, Gonen M, Rubin D, Radzyner M, Brennan MF. Long-term survival is superior after resection for cancer in high-volume centers. Ann Surg 2005;242:540-4.
8. Hirata K, Sato T, Mukaiya M, Yamashiro K, Kimura M, Sasaki K, et al. Results of 1001 pancreatic resections for invasive ductal adenocarcinoma of the pancreas. Arch Surg 1997; 132:771-6.
9. Imaizumi T, Hanyu F, Harada N, Hatori T, Fukuda A. Extended radical Whipple resection for cancer of the pancreatic head: operative procedure and results. Dig Surg 1998; 15:299-307.
10. Kawai M, Tani M, Terasawa H, Ina S, Hirono S, Nishioka R, et al. Early removal of prophylactic drains reduces the risk of intra-abdominal infections in patients with pancreatic head resection: prospective study for 104 consecutive patients. Ann Surg 2006;244:1-7.
11. Kasuaya H, Nakao A, Nomoto S, Hosono J, Takeda S, Kaneko T, et al. Postoperative delayed emptying in pylorus-preserving pancreatoduodenectomy using pancreaticogastrostomy: comparison of the reconstruction position. Hepatogastroenterology 1997;44:856-60.
12. Tani M, Terasawa H, Kawai M, Ina S, Hirono S, Uchiyama K, et al. Improvement of delayed gastric emptying in pylorus-preserving pancreaticoduodenectomy: results of a prospective, randomized, controlled trial. Ann Surg 2006; 243:316-20.
13. Tani M, Kawai M, Yamaue H. Intraabdominal hemorrhage after a pancreatectomy. J Hepatobiliary Pancreat Surg 2008;15:257-61.
14. Miura F, Asano T, Amano H, Yoshida M, Toyota N, Wada K, et al. Management of postoperative arterial hemorrhage after pancreato-biliary surgery according to the site of bleeding: relaparotomy or interventional radiology. J Hepatobiliary Pancreat Surg 2009;16:56-63.
15. Matsuno S, Egawa S, Fukuyama S, Motoi F, Sunamura M, Isaji S, et al. Pancreatic cancer registry in Japan. Pancreas 2004;28:219-30.
16. Bassi C, Dervenis C, Butturini G, Fingerhut A, Yeo C, Izbicki J, et al. Postoperative pancreatic fistula: an international study group (ISGPF) definition. Surgery 2005;138:8-13.
17. Iannitti DA, Coburn NG, Somberg J, Ryder BA, Monchik J, Cioffi WG. Use of the round ligament of the liver to decrease pancreatic fistulas: a novel technique. J Am Coll Surg 2006;203:857-64.
18. Abe N, Sugiyama M, Suzuki Y, Yanagida O, Masaki T, Mori T, et al. Falciform ligament in pancreatoduodenectomy for protection of skeletonized and divided vessels. J Hepatobiliary Pancreat Surg 2009;16:184-8.
19. Kurosaki I, Hatakeyama K. Omental wrapping of skeletonized major vessels after pancreaticoduodenectomy. Int Surg 2004;89:90-4.
20. Maeda A, Ebata T, Kanemoto H, Matsunaga K, Bando E, Yamaguchi S, et al. Omental flap in pancreaticoduodenectomy for protection of splanchnic vessels. World J Surg 2005;29:1122-6.
21. Wente MN, Bassi C, Dervenis C, Fingerhut A, Gouma DJ, Izbicki JR, et al. Delayed gastric emptying (DGE) after pancreatic surgery: a suggested definition by the International Study Group of Pancreatic Surgery (ISGPS). Surgery 2007;142:761-8.
22. Wente MN, Veit JA, Bassi C, Dervenis C, Fingerhut A, Gouma DJ, et al. Postpancreatectomy hemorrhage (PPH): an International Study Group of Pancreatic Surgery (ISGPS) definition. Surgery 2007;142:20-5.

Cancer Science
The official journal of the Japanese Cancer Association

Coexpression of MUC16 and mesothelin is related to the invasion process in pancreatic ductal adenocarcinoma

Atsushi Shimizu,[1] Seiko Hirono,[1,4] Masaji Tani,[1] Manabu Kawai,[1] Ken-Ichi Okada,[1] Motoki Miyazawa,[1] Yuji Kitahata,[1] Yasushi Nakamura,[2] Tetsuo Noda,[3] Shozo Yokoyama[1] and Hiroki Yamaue[1]

[1]Second Department of Surgery; [2]Department of Clinical Laboratory Medicine, Wakayama Medical University, Wakayama; [3]Cancer Institute, Japanese Foundation for Cancer Research, Tokyo, Japan

(Received November 18, 2011/Revised December 27, 2011/Accepted December 28, 2011/Accepted manuscript online February 9, 2012/Article first published online February 23, 2012)

The invasion process is a crucial step for pancreatic ductal adenocarcinoma (PDAC); however, the genes related to invasion remain unclear. To identify specific genes for the invasion process, we compared microarray data for infiltrating cancer and PanIN-3, which were harvested from an individual PDAC patient by microdissection. Furthermore, immunohistochemical, coimmunoprecipitation and invasion analyses were performed to confirm the biologic significance of molecules identified by expression profile. In the present study, we focused on MUC16 and mesothelin among 87 genes that were significantly upregulated in infiltrating components compared to PanIN-3 in all PDAC patients, because MUC16 was the most differently expressed between two regions, and mesothelin was reported as the receptor for MUC16. Immunohistochemical analysis revealed that MUC16 and mesothelin were expressed simultaneously only in infiltrating components and increased at the invasion front, and binding of MUC16 and mesothelin was found in PDAC by immunoprecipitation assay. The downregulation of MUC16 by shRNA and the blockage of MUC16 binding to mesothelin by antibody inhibited both invasion and migration of pancreatic cancer cell line. MUC16 high/mesothelin high expression was an independent prognostic factor for poor survival in PDAC patients. In conclusion, we identified two specific genes, MUC16 and mesothelin, associated with the invasion process in patients with PDAC. (*Cancer Sci* 2012; 103: 739–746)

For most patients with pancreatic ductal adenocarcinoma (PDAC), the diagnosis is made at an advanced stage;[1] the survival rate for these patients is dismal because PDAC has a propensity for early local invasion and vascular dissemination.[2] The genetic and biochemical determinants of the process of invasion and metastasis in PDAC are still largely unknown.

Pancreatic ductal adenocarcinoma appears to arise from histologically well-defined precursor lesions in the ducts of the pancreas, called pancreatic intraepithelial neoplasms (PanIN).[3,4] PanIN are graded based on their degree of architectural and nuclear atypia and are categorized into a four-tier classification, including PanIN-1A, 1B, 2 and 3.[5] PanIN-3 lesions demonstrate widespread loss of nuclear polarity, nuclear atypia and frequent mitoses, and whereas cancerous cells break through the basement membrane, they evolve into infiltrating adenocarcinoma. The invasion process is the crucial step in PDAC because cancer cells that invade the vasculature, or lymphatic or neural vessels, can progress further to metastasis only after obtaining infiltrating status. In the present study, we identified specific molecular markers associated with invasion in PDAC, which might be useful not only as early diagnostic markers but also as new therapeutic targets for patients with PDAC.

Several molecular markers, including tissue plasminogen activator,[6] artemin[7] and RhoGDI2,[8] have been reported to be associated with invasion in PDAC. However, some of these molecular markers are of little clinical value as therapeutic targets for patients with PDAC because these genes are also expressed in normal pancreatic tissues or other normal organs.[6–8] In this study, we first used a gene expression profiling technique to identify the specific genes that are differentially expressed between infiltrating cancer cells and PanIN-3 cells, which were harvested from an individual patient by laser microdissection. Based on our gene expression array data, clinical and biologic implications of MUC16 and mesothelin expression were further explored.

Material and Methods

Patients. Our study population included 103 patients with PDAC who underwent curative resection between January 2004 and December 2007 at Wakayama Medical University Hospital (WMUH). Informed consent was obtained from all patients in accordance with the guidelines of the Ethical Committee on Human Research of WMUH. Patient characteristics are presented in Table 1. The TNM staging criteria of the International Union Against Cancer was used for histologic classification.[9] None of the patients had received neoadjuvant chemotherapy or radiation therapy before surgery. The median follow-up duration after resection was 16.8 months (range: 1.6–67.3 months).

Laser microdissection and RNA extraction. Tissue samples including cancer cells and adjacent normal cells were embedded in Tissue-Tek OCT compound (Sakura Finetek, Torrance, CA, USA) by freezing tissue blocks in liquid nitrogen immediately after surgical resection for expression profiling. We used the tissues obtained from five patients with PDAC who had coexisting infiltrating cancer cells and PanIN-3 cells, and used the tissues from three patients as controls, including two patients with pancreatitis and one patient with bile duct cancer.

The specimens were cut into 9-μm sections at −20°C with the use of a LEICA cryostat (model 3050S; Leica, Tokyo, Japan) and then fixed on slides in 70% ethanol and stained with hematoxylin. The infiltrating cancer cells and PanIN-3 cells were harvested separately from an individual PDAC tissue using laser microdissection. As a control, the normal pancreatic duct cells were also obtained by laser microdissection, because PDAC originates from pancreatic ductal epithelial cells. Before laser microdissection, two pathologists (YS and

[4]To whom correspondence should be addressed.
E-mail: seiko-h@wakayama-med.ac.jp

doi: 10.1111/j.1349-7006.2012.02214.x

Table 1. Patient characteristics (n = 103)

Age, median (range)	69 (31–87)
Gender, male/female	54/49
Tumor site, Ph/Pbt/Phbt	71/30/2
Surgical technique, PD/DP/TP	71/30/2
Differentiation, well/moderate/poor	42/51/10
Tumor size	
≤20mm	18
>20 but ≤40mm	69
>40 but ≤60mm	14
>60mm	2
UICC stage	3
IA	3
IB	5
IIA	24
IIB	63
III	1
IV	7
Postoperative recurrence, yes/no	79/24

DP, distal pancreatectomy; Pbt, pancreatic body and tail; PD, pancreatoduodenectomy; Ph, pancreatic head; TP, total pancreatectomy; UICC, Union for International Cancer Control.

YN) diagnosed infiltrating cancer regions and PanIN-3 regions in the PDAC tissues, and normal pancreatic epithelium in normal pancreatic tissues. We estimated that the proportion of infiltrating cancer cells, PanIN-3 cells, or normal pancreatic ductal cells in the laser microdissected purified samples was at least 95%. Hence, we required more than 30 specimens (range, 35–78 specimens) in each sample for infiltrating cancer cells, more than 110 specimens (range, 111–414 specimens) for PanIN-3 cells and more than 450 specimens (range, 450–520 specimens) for normal pancreatic ductal epithelium cells to obtain enough RNA volume to use for our expression analysis. Total RNA was extracted from the harvested cells using the RNeasy Micro Kit (Qiagen, Hilden, Germany). The concentration of each total RNA sample was measured with a Nanodrop ND-1000 spectrophotometer (Nanodrop Technologies, Wilmington, DE, USA). The integrity of the RNA was determined by capillary electrophoresis using an Agilent 2100 Bioanalyzer (Agilent, Santa Clara, CA, USA) and the extracted RNA was accepted for experiments if the RNA integrity reading was >7.0.

Genome-wide transcriptional profiling. The gene expression was analyzed with Human Genome U133 Plus 2.0 GeneChips (Affymetrix, Santa Clara, CA, USA). The manufacturer's instructions regarding the protocols and the use of reagents for hybridization, washing and staining were followed (as previously described).[10] Data were collected using an Affymetrix GeneChip Scanner 3000 instrument. The cell intensity data files were obtained using the Affymetrix Suite 5.0 software program; then, the array data were imported into a DNA-Chip Analyzer (dChip, http://www.dchip.org) for high-level analysis.

Immunohistochemistry. Pretreatment was performed in a microwave using citrate buffer (pH 6.0) for 5 × 3 min at 700 W. Endogenous peroxidase activity was blocked with 3% hydrogen peroxide in methanol, and nonspecific binding sites were blocked with 10% normal goat serum. Primary antibodies were diluted in PBS: MUC16 (1:1000, mouse monoclonal, X325, Abcam, Cambridge, UK) and mesothelin (1:20, mouse monoclonal, 5B2, Novacastra, Newcastle upon Tyne, UK). Diluted primary antibodies were added, and samples were incubated overnight at 4°C. Antibody binding was then immunodetected using the avidin–biotin–peroxidase complex, as described by the supplier (Nichirei, Tokyo, Japan). Finally, the reaction products were demonstrated using a DAB substrate, and then counterstained with hematoxylin, dehydrated with ethanol and fixed with xylene.

To investigate the localization of the MUC16 and mesothelin, fluorescence immunohistochemistry was performed for paraffin-embedded tissue slides. Double labeling of the two mouse monoclonal antibodies (MUC16 [X325] and mesothelin [5B2]) was done using a Zenon kit (Molecular Probes, Eugene, OR, USA) to directly label the antibodies with either Alexa Fluor 488 or 594 according to the manufacturer's instructions.

Evaluation of immunohistochemistry. For scoring assessment, 200 cells were counted in each of the five different fields with high magnification, ×400, on the maximum cut surface of the tumor. We used ovarian cancer tissue and mesothelioma tissue as positive controls for MUC16 and mesothelin expression, respectively. The staining intensity was defined as follows: 0, no staining; 1+, weak; 2+, moderate; 3+, strong, based on the intensity levels of positive control being taken as 3+ (Fig. 1A).[11–13] If there were areas with a variety of staining intensities, the predominant intensity was chosen. The quantification of positivity (0–100%) was based on an estimate of the percentage of stained cancer cells in the lesion. The final immunostaining scores were calculated by multiplying the staining intensity and percentage positivity, thereby giving immunostaining scores ranging from 0 to 300.[14–17] The cut-off values of immunostaining scores were set as the median value, in accordance with previous reports.[18,19] The immunostains were scored by three investigators (SH, YN and HY) blinded to the clinical and pathologic data. If differences of opinion arose, a consensus was achieved by discussion.

Cell lines and RNA interference. Human pancreatic cancer cell line PK9 was obtained from the Cell Resource Center for Biomedical Research Institute of Development, Tohoku University (Miyagi, Japan).

Short hairpin RNA (shRNA) plasmids designed to target MUC16 were synthesized by SA Biosciences (Frederick, MD, USA) as follows: insert sequence ACAGCAGCATCAAGAGTTATT and ggaatctcattcgatgcatac (negative control). Each plasmid (0.8 μg) was mixed with 1 μL Lipofectamine2000 (Invitrogen, Carlsbad, CA, USA) in a final volume of 100 μL of Opti-MEM medium and was added to PK9 cells grown to 40% confluence in 24-well plates. Forty-eight hours after transfection, G418 solution (Roche, Basel, Switzerland) was added in the appropriate concentration. The stably transfected cells were maintained in RPMI-1640.

Coimmunoprecipitation assay. To address binding between MUC16 and mesothelin, we performed coimmunoprecipitation assays using pancreatic cancer cell line PK9 and two surgical specimens obtained from 2 PDAC patients. The coimmunoprecipitation assays were performed using the Universal Magnetic Co-IP Kit (Active Motif, Rixensart, Belgium) according to the manufacturer's protocol. Monoclonal antibody against CA125 (OC125, Abcam, Cambridge, UK), monoclonal antibody against mesothelin (MN-1, Rockland, Gilbertsville, PA, USA) or rabbit IgG control (Abcam) were used for immunoprecipitation and immunoblotting.

***In vitro* invasion and migration assay in PK9 cell line transfected with MUC16 shRNA.** To investigate the effect of MUC16 expression on invasion and migration of pancreatic cancer cells, *in vitro* invasion and migration assays were performed in the membrane culture system using an 8-μm pore size PET membrane coated with or without Matrigel (24-well, BD Biosciences, San Diego, CA, USA). Parental PK9 cells, vector control-PK9 cells and PK9 cells transfected with MUC16 shRNA were seeded into 5 × 10^4 cells/500 μL growth medium on the Matrigel layer. The following procedures were performed (as previously described).[20]

doi: 10.1111/j.1349-7006.2012.02214.x

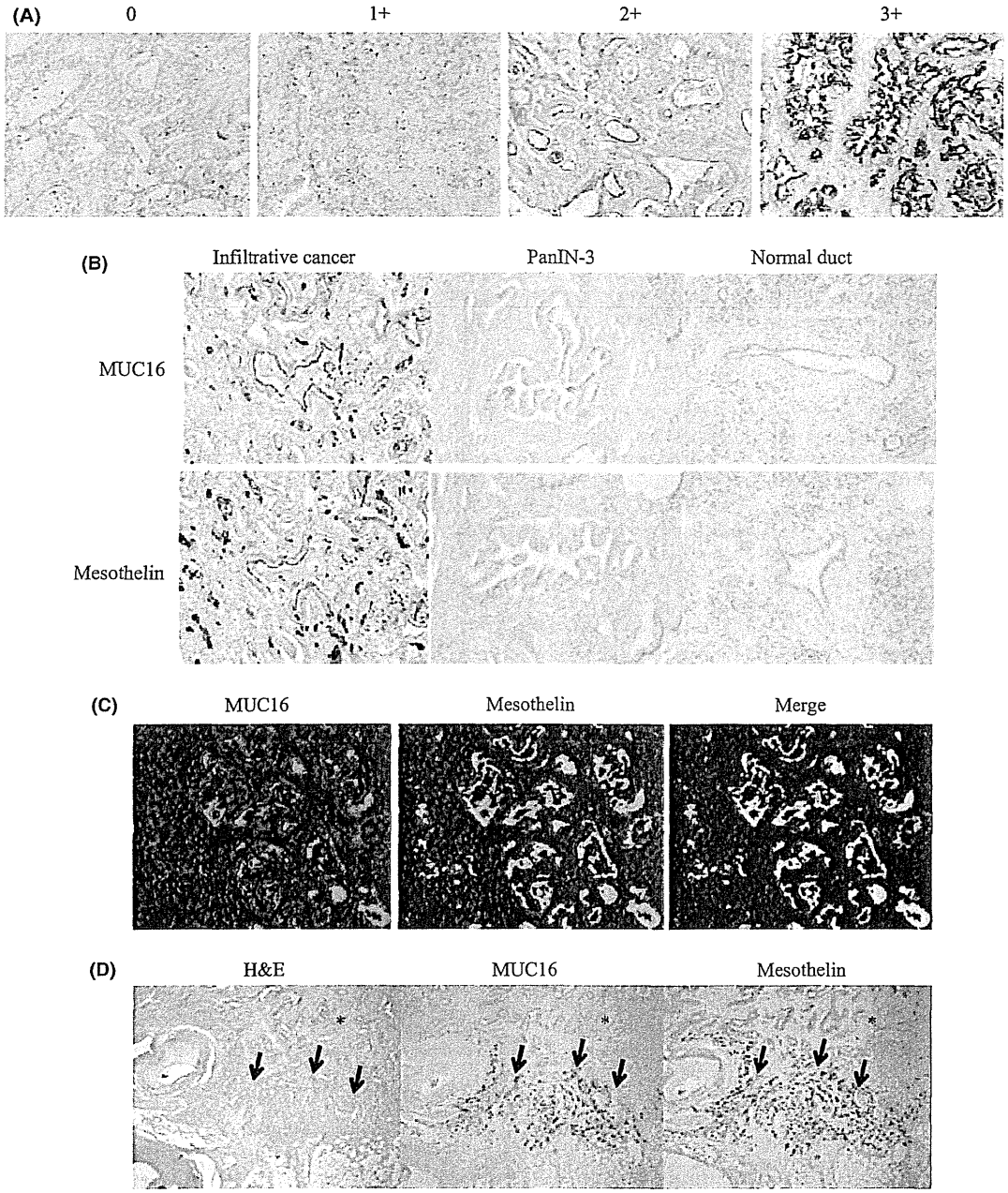

Fig. 1. (A) Image of staining intensity grade. (0) no staining, (1+) weak, (2+) moderate, (3+) strong intensity. (B) MUC16 and mesothelin were stained at the apical membrane or cytoplasm only in infiltrative cancer, whereas no staining appeared in PanIN-3 cells and normal ductal cells. (C) MUC16 and mesothelin expressed at the apical cancer cell surface in invasive ductal cancer cells labeled with Zenon Alexa Fluor 594 and 488. The merged image shows MUC16 and mesothelin expressed in the same cancer cells simultaneously. (D) The expression of MUC16 and mesothelin was higher at the invasion front (arrow) than in the main tumor (*). H&E, hematoxylin and eosin stain.

***In vitro* invasion and migration assays with blocking antibodies for MUC16 and mesothelin.** To investigate the binding between MUC16 and mesothelin, we evaluated the effect of blocking antibodies against interaction between MUC16 and mesothelin on invasion and migration of pancreatic cancer cell PK9 by using *in vitro* invasion and migration assay. Because OC125 (DAKO, Carpinteria, CA, USA) and M11 (DAKO) are known to block the interaction between MUC16 and mesothelin,[21] each antibody was used for blocking the interaction. Sodium azide was removed using the AbSelect Antibody Purification System (Innova Biosciences, Cambridge, UK).

Statistical analysis. The association between MUC16/mesothelin expression and clinicopathologic factors in the patients with PDAC was assessed using the χ^2-test or the Fisher exact test. The survival curves were calculated using the Kaplan–Meier method and then compared by means of the log-rank test. The prognostic significance of clinicopathologic features and MUC16/mesothelin expression was determined using univariate Cox regression analysis. Cox proportional hazards models were fitted for multivariate analysis. Statistical procedures were performed using SPSS version 13.0 (SPSS, Chicago, IL, USA). $P < 0.05$ was considered statistically significant.

Results

Identification of the transcriptional biomarkers associated with the invasion of pancreatic ductal adenocarcinoma by gene expression profiling. Microarray data for the infiltrating cancer and PanIN-3, which were harvested from an individual PDAC patient, were compared on the basis of the following criteria: (i) a ≥ 1.5-fold change in the expression levels between the infiltrating cells and PanIN-3 cells; (ii) a >100 absolute difference between the expression levels of the infiltrating cells and PanIN-3 cells; and (iii) $P < 0.05$.[22,23] A total of 109 genes were differentially expressed between infiltrating cancer and PanIN-3 cells in PDAC, including 87 genes that were upregulated and 22 that were downregulated in the infiltrating PDAC, and then 18 genes, which were expressed more in both infiltrating cancer and PanIN3 than in normal pancreatic epithelium, were listed (see Table 2), to focus on more significant genes related to carcinogenesis in PDAC. Among the upregulated genes identified by expression profiling, we focused on MUC16 because MUC16 expression in the infiltrating cancer was substantially higher than that of the PanIN-3 cells in all five PDAC patients and normal pancreatic duct epithelium (Table 2), indicating that MUC16 is specifically expressed in invasive PDAC. We also focused on mesothelin in the upregulates genes list, because it had been previously reported to be a ligand receptor of MUC16.[24,25]

Immunohistochemical staining of MUC16 and mesothelin in pancreatic ductal adenocarcinoma. The immunohistochemical analyses were performed in the paraffin-embedded tissues from 103 patients with PDAC. MUC16 and mesothelin were stained by immunohistochemistry at the tumor apical membrane or cytoplasm (or both) in PDAC samples (Fig. 1B). Both MUC16 and mesothelin were expressed only in the infiltrating cancer cells and not in the PanIN-3 cells ($n = 30$) or normal pancreatic epithelial cells ($n = 103$) (Fig. 1B). Furthermore, we found that these genes were not expressed in any non-epithelial cells, including stromal cells, acinar cells and islet cells. Fluorescence immunohistochemistry using the merge technique showed that MUC16 and mesothelin were stained in the same cancer cells simultaneously (Fig. 1C). We observed that MUC16 and mesothelin were more highly expressed at the invasion front than in the main tumor in 48 of the 103 patients (47%) with PDAC (Fig. 1D).

The scores of MUC16 and mesothelin expression were calculated for each sample. The median scores of MUC16 and mesothelin were 150 (range, 0–300) and 180 (range, 0–300), respectively. The binarization of the score data for these markers was performed as "high expression" versus "low expression" at the median level. We categorized all samples into two groups to analyze the association of MUC16 and mesothelin expression with the clinicopathologic features in the patients with PDAC: the MUC16 high/mesothelin high expression group ($n = 41$) versus the other group ($n = 62$), which included the patients with MUC16 high/mesothelin low expression ($n = 11$), those with MUC16 low/mesothelin high expression ($n = 11$) and MUC16 low/mesothelin low expression ($n = 40$).

Association of MUC16 and mesothelin expression with pathologic factors. The correlation of pathologic factors and MUC16/mesothelin expression was analyzed (Table 3). These pathologic factors were evaluated in accordance with the second English edition of the Classification of Pancreatic Carcinoma, proposed by the Japan Pancreas Society.[26] The analysis indicated that a tumor size >4.0 cm, serosal invasion, invasion of other organs, and lymphatic permeation occurred significantly more often in the MUC16 high/mesothelin high expression group than in the other groups ($P = 0.0041$, $P = 0.0131$, $P = 0.0356$ and $P = 0.0250$, respectively).

Binding of MUC16 and mesothelin in pancreatic cancer cell PK9 and surgical specimens from patients with pancreatic ductal adenocarcinoma. The coimmunoprecipitation assays between MUC16 and mesothelin using pancreatic cancer cell line PK9 and surgical specimens obtained from two PDAC patients (number 1: stage IIB, number 2: stage IV) showed that the whole cell lysates or tissue homogenates were immunoprecipitated and immunoblotted with anti-MUC16 and anti-mesothelin antibody (Fig. 2A), indicating that MUC16 and mesothelin can bind in PDAC.

Role of MUC16 and mesothelin in invasion, migration and cell growth of pancreatic cancer cell line. PK9 cells express MUC16 and were transfected with shRNA targeted to MUC16. Stable

Table 2. Upregulated genes in the infiltrating cancer compared to PanIN-3 component of pancreatic ductal adenocarcinoma as determined by expression profiling

Probe ID	Gene name	Gene symbol	Fold change, mean	Mean expression level	
				IC/PanIN-3	IC/normal
220196_at	Mucin 16	MUC16	26.7	14.6	31.6
206884_s_at	Sciellin	SCEL	17.4	3.8	4.7
205388_at	Troponin C type 2	TNNC2	10.1	4.1	10.0
204416_x_at	Apolipoprotein C-I	APOC1	6.7	5.9	7.2
213524_s_at	G0/G1switch 2	G0S2	5.4	4.3	13.9
202504_at	Tripartite motif-containing 29	TRIM29	4.5	2.6	8.8
204070_at	Retinoic acid receptor responder 3	RARRES3	3.7	3.4	5.4
242625_at	Radical S-adenosyl methionine domain containing 2	RSAD2	3.6	2.4	12.1
204885_s_at	Mesothelin	MSLN	3.0	2.2	2.2
201564_s_at	Fascin homolog 1, actin-bundling protein	FSCN1	3.0	2.7	3.1
205483_s_at	Interferon, alpha-inducible protein	IFI	3.0	2.5	7.6
228640_at	BH-protocadherin	PCDH7	2.7	2.5	7.5
239979_at	Epithelial stromal interaction 1	EPSTI1	2.5	2.1	6.5
231956_at	KIAA1618	KIAA1618	2.4	2.4	3.8
204285_s_at	Phorbol-12-myristate-13-acetate-induced protein 1	PMAIP1	2.2	2.1	3.4
222810_s_at	RAS protein activator like 2	RASAL2	2.2	2.2	2.3
243271_at	Sterile alpha motif domain containing 9-like	SAMD9L	2.1	1.9	5.7
200736_s_at	Glutathione peroxidase 1	GPX1	2.0	1.9	2.0

IC, infiltrating cancer; PanIN, pancreatic intraepithelial neoplasms.

doi: 10.1111/j.1349-7006.2012.02214.x

Table 3. The association of MUC16 and mesothelin expression with pathologic factors in patients with pancreatic ductal adenocarcinoma

	Number	MUC16 high/ mesothelin high group	Other group	*P*
		41	62	
Differentiation				
Well/ moderate	93	35	57	0.1908
Poor	10	6	4	
Tumor size				
>40mm	16	12	4	0.0041
≤40mm	87	29	58	
Local progression				
Intrapancreatic common bile duct invasion				
Positive	22	6	16	0.1757
Negative	81	35	46	
Duodenal invasion				
Positive	40	12	28	0.1052
Negative	63	29	34	
Serosal invasion				
Positive	74	35	39	0.0131
Negative	29	6	23	
Retropancreatic tissue invasion				
Positive	85	35	50	0.5369
Negative	18	6	12	
Portal venous system invasion				
Positive	25	13	12	0.1523
Negative	78	28	50	
Arterial system invasion				
Positive	5	4	1	0.0803
Negative	98	37	61	
Extrapancreatic nerve plexus invasion				
Positive	33	16	17	0.2166
Negative	70	25	45	
Invasion of other organs				
Positive	6	5	1	0.0356
Negative	97	36	61	
Lymphatic permeation				
Positive	88	39	49	0.0250
Negative	15	2	13	
Vascular permeation				
Positive	64	28	36	0.2948
Negative	39	13	26	
Perineural invasion				
Positive	76	29	47	0.5665
Negative	27	12	15	
Lymph node metastasis				
Positive	69	32	37	0.0523
Negative	34	9	25	

MUC16–shRNA-transfected PK9 cells showed downregulation of MUC16 protein expression compared to the vector control (data not shown). Invasion chamber experiments revealed that MUC16–shRNA-transfected PK9 cells had significant suppression of cell invasion (Fig. 2B). Migration assays also demonstrated that downregulation of MUC16 significantly reduced migration (Fig. 2C). The blockage of MUC16 binding to mesothelin with the neutralizing antibodies against MUC16 (OC125 or M11) significantly suppressed invasion and migration of pancreatic cancer cells (Fig. 2D,E). In terms of the effect of MUC16 on cell growth, parental PK9 cells, vector control-PK9 cells and MUC16–shRNA-transfected PK9 were seeded in concentration of 10×10^4/mL, and the cell numbers were counted on day 1, 3 and 5 using a hemocytometer. As a result, the cell growth was significantly suppressed after inhibition of MUC16 expression (Fig. 2F).

Association of MUC16 and mesothelin expression with survival in patients with pancreatic ductal adenocarcinoma. The overall survival of the MUC16 high/mesothelin high expression group was significantly worse than in the other group (median 11.9 *vs* 22.8 months, $P = 0.0006$; Fig. 3A). The 1-, 3- and 5-year survival rates of the MUC16 high/mesothelin high group versus the other group were as follows: 51.2 *vs* 72.6%, 8.0 *vs* 25.6% and 0 *vs* 11.5%, respectively. The disease-free survival of the MUC16 high/mesothelin high expression group was also worse than the other group (median 6.7 *vs* 10.9 months, $P = 0.0002$; Fig. 3B). The 1-, 3- and 5-year disease-free survival rates of the MUC16 high/mesothelin high group versus the other group were as follows: 12.2 *vs* 48.4%, 2.5 *vs* 20.3% and 0 *vs* 11.5%, respectively. In the univariate analysis of the overall survival of the patients with PDAC, a tumor size > 4.0 cm, duodenal invasion, portal venous system invasion, lymphatic permeation, vascular permeation, lymph node metastasis and MUC16 high/mesothelin high expression were potential factors for predicting poor survival (Table 4). According to a multivariate analysis of overall survival, vascular permeation and MUC16 high/mesothelin high expression were independent factors for predicting short survival for the patients with PDAC ($P = 0.0025$, HR, 2.241; 95% CI, 1.364–4.310; $P = 0.0158$, HR, 1.936; 95%CI, 1.132–3.310, respectively; Table 4). Similarly, in the multivariate analysis of disease-free survival, a tumor size > 4.0 cm, lymphatic permeation and MUC16 high/mesothelin high expression were independent prognostic factors for a poorer disease-free survival ($P = 0.0167$, HR, 2.141, 95% CI, 1.148–4.000; $P = 0.0202$, HR, 3.984, 95% CI, 1.241–12.821; $P = 0.0131$, HR, 1.985, 95% CI, 1.155–3.412, respectively; Table 5).

Discussion

We first identified genes specific to the invasion process in PDAC using microdissection and gene expression profiling techniques. In this study, we compared microarray data of infiltrating cancer and PanIN3, which were harvested from an individual PDAC patient, to exclude the difference in original gene expression among individuals. Then, we were able to identify similar genes that were differently expressed between infiltrating cancer and PanIN-3 in all five patients.

Among the identified upregulated genes, we focused on MUC16 because its expression in the infiltrating cancer was substantially higher than that in the PanIN-3 cells. We also focused on mesothelin in the list, because it was reported to be a ligand receptor of MUC16. Their interaction has been postulated to play an important role during tumorigenesis and metastasis in ovarian cancer.[24,25] Rump and colleagues reported that the binding of MUC16 and mesothelin expressed by cancer cells mediates heterotypic cell adhesion and might contribute to the metastasis and invasion of ovarian cancer.[24]

In the present study, immunohistochemical analysis revealed that MUC16 and mesothelin were expressed in the infiltrating cancer cells but not in the PanIN-3 cells or normal pancreatic tissues, consistent with the results of gene expression profiling. Furthermore, fluorescence immunohistochemistry showed that MUC16 and mesothelin were expressed simultaneously in the PDAC cells.

MUC16 encodes the CA125 antigen and is a membrane-bound mucin protein with a high molecular weight between 2.5 and 5.0 million daltons.[27] Its proposed structure comprises an N-terminal domain of >22 000 amino acid residues that are presumably heavily glycosylated, a central domain containing up to 60 glycosylated repeat sequences constituting

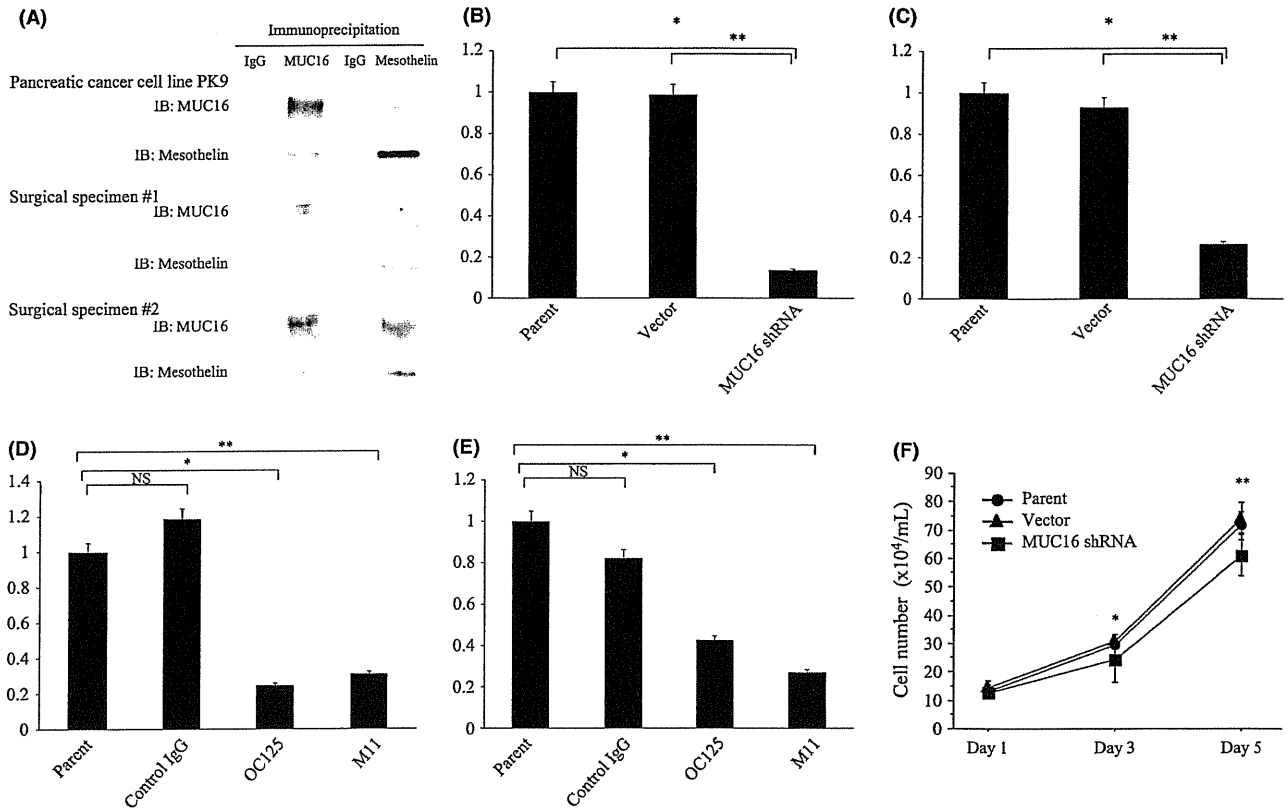

Fig. 2. (A) The results of coimmunoprecipitation assay in pancreatic cancer cell line PK9 and clinical samples from the patients with pancreatic ductal adenocarcinoma. The whole cell lysates extracted from cell line or tissue homogenates extracted from two surgical specimens were immunoprecipitated and immunoblotted with anti-MUC16 and anti-mesothelin antibody. IB, immunoblotting. (B) Invasion chamber experiments in PK9 transfected with MUC16 shRNA. The invasion was significantly suppressed after inhibition of MUC16 expression (*P = 0.0009, **P = 0.0067). (C) Migration assays in PK9 transfected with MUC16 shRNA. The migration was significantly suppressed after downregulation of MUC16 expression (*P = 0.0005, **P = 0.0055). (D) Invasion assay with the blockage of MUC16 binding to mesothelin with the neutralizing antibodies against MUC16 (OC125 or M11, *P = 0.0014, **P = 0.0043). (E) Migration assay with the blockage of MUC16 binding to mesothelin with OC12 5 or M11 (*P = 0.0020, **P = 0.0003). (F) Cell growth assay in PK9 transfected with MUC16 shRNA. The cell growth was significantly suppressed after inhibition of MUC16 expression (*P = 0.0469, **P = 0.0036). NS, not significant.

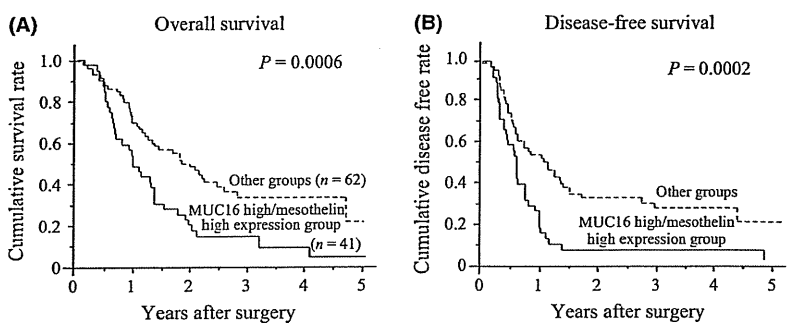

Fig. 3. The overall survival (A) and disease-free survival (B) of the MUC16 high/mesothelin high expression group was worse than that of the other groups (median, 11.9 *vs* 22.8 months, P = 0.0006; 6.7 *vs* 10.9 months, P = 0.0002, respectively).

the tandem repeats characteristic of mucins, and a C-terminal domain composed of a transmembrane domain and a short cytoplasmic tail with possible phosphorylation sites.[28] Few reports have described the expression of MUC16 in cancers. In this study, using immunohistochemistry, we detected the expression of MUC16 in 94 of 103 PDAC cases (91%).

The mesothelin gene encodes a 71-kDa precursor protein that is processed into the 40-kDa glycosylphosphatidylinositol-anchored membrane glycoprotein, mesothelin and a 31-kDa fragment called megakaryocyte potentiating factor.[29,30] Mesothelin expression in normal human tissues is limited to mesothelial cells lining the pleura, pericardium and peritoneum,[29] and the protein is also expressed by a variety of solid tumors, including ovarian cancer, malignant mesothelioma, lung cancer and PDAC.[31,32] Mesothelin expression reportedly conferred chemoresistance and a poorer clinical outcome in ovarian cancer patients.[33]

We found that the coexpression of MUC16 and mesothelin was also increased at the invasion front (n = 48), compared to that in the main tumor in several PDAC tissues, and, then, MUC16 high/mesothelin high expression in PDAC was significantly associated with large tumors, serosal invasion, invasion of other organs and lymphatic permeation. These results indicate that these molecules seem to be involved in invasion and

doi: 10.1111/j.1349-7006.2012.02214.x

Table 4. Univariate and multivariate analysis using the Cox proportional hazards regression model of overall survival in 103 patients with pancreatic ductal adenocarcinoma

	Univariate analysis			Multivariate analysis		
	P	HR	95% CI	*P*	HR	95% CI
Age, ≥70	0.2692	0.906	0.962–1.011	–	–	–
Gender, male	0.7711	1.026	0.678–1.689	–	–	–
Differentiation, poor	0.9228	1.043	0.451–2.410	–	–	–
Tumor size, > 40 mm	0.0070	2.203	1.241–3.906	0.3294	1.340	0.743–2.421
Local progression						
CH, positive	0.1651	1.458	0.856–2.481	–	–	–
DU, positive	0.0465	1.595	1.007–2.525	0.0782	1.575	0.950–2.604
S, positive	0.3320	1.297	0.767–2.188	–	–	–
RP, positive	0.0715	1.848	0.948–3.610	–	–	–
PV, positive	0.0203	1.818	1.098–3.012	0.6830	1.119	0.653–1.916
A, positive	0.6183	1.259	0.507–3.135	–	–	–
PL, positive	0.0666	1.543	0.971–2.451	–	–	–
OO, positive	0.4899	1.342	0.581–3.101	–	–	–
Lymphatic permeation, positive	0.0034	3.937	1.575–9.804	0.1190	2.375	0.801–7.042
Vascular permeation, positive	< 0.0001	3.155	1.859–5.348	0.0025	2.421	1.364–4.310
Perineural invasion, positive	0.1345	1.527	0.877–2.660	–	–	–
Lymph node metastasis, positive	0.0043	2.151	1.272–3.636	0.8436	1.067	0.561–2.033
MUC16/mesothelin expression, high	0.0008	2.206	1.392–3.495	0.0158	1.936	1.132–3.310

A, arterial system invasion; CH, intrapancreatic common bile duct invasion; CI, confidence interval; DU, duodenal invasion; HR, hazard ratio; OO, invasion of other organs; PL, extrapancreatic nerve plexus invasion; PV, portal venous system invasion; RP, retropancreatic tissue invasion; S, serosal invasion.

Table 5. Univariate and multivariate analysis using the Cox proportional hazards regression model of disease-free survival in 103 patients with pancreatic ductal adenocarcinoma

	Univariate analysis			Multivariate analysis		
	P	HR	95% CI	*P*	HR	95% CI
Age, ≥70	0.5105	1.161	0.743–1.815	–	–	–
Gender, male	0.9862	0.996	0.638–1.555	–	–	–
Differentiation, poor	0.5830	0.792	0.344–1.825	–	–	–
Tumor size, > 40 mm	0.0001	3.257	1.770–5.988	0.0167	2.141	1.148–4.000
Local progression						
CH, positive	0.6377	1.138	0.664–1.953	–	–	–
DU, positive	0.0105	1.805	1.148–2.833	0.0633	1.590	0.975–2.591
S, positive	0.0864	1.605	0.935–2.755	–	–	–
RP, positive	0.1104	1.689	0.887–3.205	–	–	–
PV, positive	0.0410	1.675	1.021–2.755	0.6492	1.136	0.656–1.965
A, positive	0.8599	1.095	0.397–3.021	–	–	–
PL, positive	0.2523	1.316	0.822–2.110	–	–	–
OO, positive	0.7087	1.189	0.479–2.959	–	–	–
Lymphatic permeation, positive	0.0034	3.937	2.370–18.181	0.0202	3.984	1.241–12.821
Vascular permeation, positive	0.0012	2.198	1.362–3.546	0.1429	1.506	0.871–2.604
Perineural invasion, positive	0.0452	1.736	1.012–2.985	0.1162	1.577	0.894–2.778
Lymph node metastasis, positive	< 0.0001	3.778	1.938–5.917	0.2388	1.484	0.770–2.857
MUC16/mesothelin expression, high	0.0002	2.378	1.497–3.777	0.0131	1.985	1.155–3.412

A, arterial system invasion; CH, intrapancreatic common bile duct invasion; CI, confidence interval; DU, duodenal invasion; HR, hazard ratio; OO, invasion of other organs; PL, extrapancreatic nerve plexus invasion; PV, portal venous system invasion; RP, retropancreatic tissue invasion; S, serosal invasion.

migration of pancreatic cancer cells. Recent reports show the role of MUC16 in ovarian cancer tumorigenesis,[34,35] and it has been noted that MUC16 regulates cell growth, invasion and metastasis in epithelial ovarian cancer.[34] However, another report indicates the opposite concept, that downregulation of MUC16 inhibits invasion and migration due to the suppression of epithelial to mesenchymal transition in ovarian cancer cells.[35] Thus, the role of MUC16 in ovarian cancer cell invasion and migration is still controversial and no report regarding the role of MUC16 on pancreatic cancer cell invasion and migration has yet appeared.

To examine the role of interaction of MUC16 and mesothelin on pancreatic cancer invasion and migration, we investigated whether shRNA and blocking antibodies for MUC16 suppress invasion and migration of pancreatic cancer cells. We investigated the expression of MUC16 and mesothelin by RT-PCR, western blotting and immunocytochemistry in eight pancreatic cancer cell lines (PK9, PANC1, MIAPaCa2, AsPC1, BxPC3, Capan-1, Capan-2 and PK1). By RT-PCR, both MUC16 and mesothelin mRNAs were detected in five cell lines, including PK9, AsPC1, BxPC3, Capan-2 and PK1. Using western blotting and immunocytochemistry, the strongest positive

expressions of both MUC16 and mesothelin were found in PK9. Therefore, in the present study, we used only PK9 cell line for biological experiments. The blockage of the interaction between MUC16 and mesothelin suppressed invasion and migration of pancreatic cancer cells, suggesting that MUC16 binding to mesothelin is important for cell invasion and migration in pancreatic cancer cells.

Furthermore, we focused on the survival of patients with MUC16 high and mesothelin high expression because coexpression of these two genes is obviously correlated to the invasion of PDAC, and MUC16 high/mesothelin high expression was an independent prognostic factor for poor survival. We examined whether there are any differences in survival between the MUC16 high/mesothelin high group and the MUC16 high/mesothelin low group or MUC16 low/mesothelin high group. However, these groups were very small (n = 11), and larger groups of patients are necessary for further study.

The mechanism of overexpression of MUC16 and mesothelin in PDAC has not yet been clarified yet. It is also unclear whether the coexpression of MUC16 and mesothelin was coincidental or the increased expression of MUC16 was associated with an upregulation of mesothelin expression. These issues should be clarified in further studies. Moreover, other molecules in Table 2 besides MUC16 and mesothelin might potentially contribute to the invasion process. In the future, we analyze the roles of other upregulated genes in infiltrating cancer than in PanIN-3 for PDAC patients.

In conclusion, MUC16 and mesothelin are involved in pancreatic cancer cell invasion and migration, and MUC16 and mesothelin clinically represent new prognostic biomarkers for PDAC and might be new therapeutic targets for patients with PDAC, including immunotherapy using a peptide vaccine or monoclonal antibody therapy.

Acknowledgments

This study was supported by Grant-in-Aid no.19390341 and 22791297 from the Ministry of Education, Culture, Sports, Science and Technology of Japan.

Disclosure Statement

The authors have no conflict of interest.

References

1 Hidalgo M. Pancreatic cancer. *N Engl J Med* 2010; **362**: 1605–17.
2 Dumartin L, Quemener C, Laklai H *et al.* Netrin-1 mediates early events in pancreatic adenocarcinoma progression, acting on tumor and endothelial cells. *Gastroenterology* 2010; **138**: 1595–606.
3 Hruban RH, Goggins M, Parsons J Kern SE. Progression model for pancreatic cancer. *Clin Cancer Res* 2000; **6**: 2969–72.
4 Hruban RH, Adsay NV, Albores-Saavedra J *et al.* Pancreatic intraepithelial neoplasia: a new nomenclature and classification system for pancreatic duct lesions. *Am J Surg Pathol* 2001; **25**: 579–86.
5 Kern S, Hruban R, Hollingsworth MA *et al.* A white paper: the product of a pancreas cancer think tank. *Cancer Res* 2001; **61**: 4923–32.
6 Diaz VM, Hurtado M, Thomson TM, Reventos J, Paciucci R. Specific interaction of tissue-type plasminogen activator (t-PA) with annexin II on the membrane of pancreatic cancer cells activates plasminogen and promotes invasion in vitro. *Gut* 2004; **53**: 993–1000.
7 Ceyhan GO, Giese NA, Erkan M *et al.* The neurotrophic factor artemin promotes pancreatic cancer invasion. *Ann Surg* 2006; **244**: 274–81.
8 Abiatari I, DeOliveira T, Kerkadze V *et al.* Consensus transcriptome signature of perineural invasion in pancreatic carcinoma. *Mol Cancer Ther* 2009; **8**: 1494–504.
9 Sobin LH, Wittekind CH. *International Union Against Cancer: TNM Classification of Malignant Tumors*, 6th edn. New York, NY: Wiley and Liss, 2002.
10 Hirono S, Yamaue H, Hoshikawa Y *et al.* Molecular markers associated with lymph node metastasis in pancreatic ductal adenocarcinoma by genome-wide expression profiling. *Cancer Sci* 2010; **101**: 259–66.
11 McClelland RA, Finlay P, Walker KJ *et al.* Automated quantitation of immunocytochemically localized estrogen receptors in human breast cancer. *Cancer Res* 1990; **50**: 3545–50.
12 Detre S, Saclani Jotti G, Dowsett M. A "quickscore" method for immunohistochemical semiquantitation: Validation for oestrogen receptor in breast carcinomas. *J Clin Pathol* 1995; **48**: 876–8.
13 Allred DC, Harvey JM, Berardo M, Clark GM. Prognostic and predictive factors in breast cancer by immunohistochemical analysis. *Mod Pathol* 1998; **11**: 155–68.
14 Campagna D, Cope L, Lakkur SS, Henderson C, Laheru D, Iacobuzio-Donahue CA. Gene expression profiles associated with advanced pancreatic cancer. *Int J Clin Exp Pathol* 2008; **1**: 32–43.
15 Fritsche P, Seidler B, Schuler S *et al.* HDAC2 mediates therapeutic resistance of pancreatic cancer cells via the BH3-only protein NOXA. *Gut* 2009; **58**: 1399–409.
16 Meinhold-Heerlein I, Stenner-Liewen F, Liewen H *et al.* Expression and potential role of Fas-associated phosphatase-1 in ovarian cancer. *Am J Pathol* 2001; **158**: 1335–44.
17 Seethala RR, Gooding WE, Handler PN *et al.* Immunohistochemical analysis of phosphotyrosine signal transducer and activator of transcription 3 and epidermal growth factor receptor autocrine signaling pathways in head and neck cancers and metastatic lymph nodes. *Clin Cancer Res* 2008; **14**: 1303–9.
18 Campbell EJ, McDuff E, Tatarov O *et al.* Phosphorylated c-Src in the nucleus is associated with improved patient outcome in ER-positive breast cancer. *Br J Cancer* 2008; **99**: 1769–74.
19 Cappia S, Righi L, Mirabelli D *et al.* Prognostic role of osteopontin expression in malignant pleural mesothelioma. *Am J Clin Pathol* 2008; **130**: 58–64.
20 Ieda J, Yokoyama S, Tamura K *et al.* Re-expression of CEACAM1 long cytoplasmic domain isoform is associated with invasion and migration of colorectal cancer. *Int J Cancer* 2011; **129**: 1351–61.
21 Scholler N, Garvik B, Hayden-Ledbetter M, Kline T, Urban N. Development of a CA125-mesothelin cell adhesion assay as a screening tool for biologics discovery. *Cancer Lett* 2007; **8**: 130–6.
22 Gronborg M, Kristiansen TZ, Iwahori A *et al.* Biomarker discovery from pancreatic cancer secretome using a differential proteomic approach. *Mol Cell Proteomics* 2006; **5**: 157–71.
23 Yamanaka S, Sunamura M, Furukawa T *et al.* Chromosome 12, frequently deleted in human pancreatic cancer, may encode a tumor-suppressor gene that suppresses angiogenesis. *Lab Invest* 2004; **84**: 1339–51.
24 Rump A, Morikawa Y, Tanaka M *et al.* Binding of ovarian cancer antigen CA125/MUC16 to mesothelin mediates cell adhesion. *J Biol Chem* 2004; **279**: 9190–8.
25 Gubbels JA, Belisle J, Onda M *et al.* Mesothelin-MUC16 binding is a high affinity, N-glycan dependent interaction that facilitates peritoneal metastasis of ovarian tumors. *Mol Cancer* 2006; **5**: 50.
26 Japan Pancreas Society. *Classification of Pancreatic Carcinoma*, 2nd English edn. Tokyo: Kanahara, 2003.
27 Yin BW, Lloyd KO. Molecular cloning of the CA125 ovarian cancer antigen: identification as a new mucin, MUC16. *J Biol Chem* 2001; **276**: 27371–5.
28 O'Brien TJ, Beard JB, Underwood LJ, Shigemasa K. The CA 125 gene: a newly discovered extension of the glycosylated N-terminal domain doubles the size of this extracellular superstructure. *Tumor Biol* 2002; **23**: 154–69.
29 Chang K, Pastan I, Willingham MC. Isolation and characterization of a monoclonal antibody, K1, reactive with ovarian cancers and normal mesothelium. *Int J Cancer* 1992; **50**: 373–81.
30 Hassan R, Bera T, Pastan I. Mesothelin: a new target for immunotherapy. *Clin Cancer Res* 2004; **10**(12 Pt 1): 3937–42.
31 Ordonez NG. Application of mesothelin immunostaining in tumor diagnosis. *Am J Surg Pathol* 2003; **27**: 1418–28.
32 Argani P, Iacobuzio-Donahue CA, Ryu B *et al.* Mesothelin is overexpressed in the vast majority of ductal adenocarcinomas of the pancreas: identification of a new pancreatic cancer marker by serial analysis of gene expression (SAGE). *Clin Cancer Res* 2001; **7**: 3862–8.
33 Cheng WF, Huang CY, Chang MC *et al.* High mesothelin correlates with chemoresistance and poor survival in epithelial ovarian carcinoma. *Br J Cancer* 2009; **100**: 1144–53.
34 Thériault C, Pinard M, Comamala M *et al.* MUC16 (CA125) regulates epithelial ovarian cancer cell growth, tumorigenesis and metastasis. *Gynecol Oncol* 2011; **121**: 434–43.
35 Comamala M, Pinard M, Thériault C *et al.* Downregulation of cell surface CA125/MUC16 induces epithelial-to-mesenchymal transition and restores EGFR signaling in NIH:OVCAR3 ovarian carcinoma cells. *Br J Cancer* 2011; **104**: 989–99.

doi: 10.1111/j.1349-7006.2012.02214.x

Hindawi Publishing Corporation
Journal of Biomedicine and Biotechnology
Volume 2012, Article ID 848042, 10 pages
doi:10.1155/2012/848042

Research Article

Identification of HLA-A24-Restricted Novel T Cell Epitope Peptides Derived from P-Cadherin and Kinesin Family Member 20A

Ryuji Osawa,[1,2] Takuya Tsunoda,[1,2,3] Sachiko Yoshimura,[1,2] Tomohisa Watanabe,[2] Motoki Miyazawa,[1] Masaji Tani,[1] Kazuyoshi Takeda,[4] Hidewaki Nakagawa,[3] Yusuke Nakamura,[3] and Hiroki Yamaue[1]

[1] *Second Department of Surgery, Wakayama Medical University, 811-1 Kimiidera, Wakayama 641-8510, Japan*
[2] *OncoTherapy Science Inc. Research Department, Kanagawa 213-0012, Japan*
[3] *Laboratory of Molecular Medicine, Human Genome Center, Institute of Medical Science, The University of Tokyo, Tokyo 108-8639, Japan*
[4] *Department of Immunology, Juntendo University School of Medicine, Tokyo 113-8421, Japan*

Correspondence should be addressed to Hiroki Yamaue, yamaue-h@wakayama-med.ac.jp

Received 6 February 2012; Revised 9 April 2012; Accepted 9 April 2012

Academic Editor: Soldano Ferrone

We here identified human leukocyte antigen-(HLA-)A*2402-restricted epitope peptides from Cadherin 3, type 1, P-cadherin (CDH3) and kinesin family member 20A (KIF20A) that were found to be specifically expressed in cancer cells through genome-wide expression profile analysis. CDH3-10-807 peptide and KIF20A-10-66 peptide successfully induced specific CTL clones, and these selectively responded to COS7 cells expressing both HLA-A*2402 and respective protein while did not respond to parental cells or COS7 cells expressing either HLA-A*2402 or respective protein. Furthermore, CTL clones responded to cancer cells that endogenously express HLA-A*2402 and respective protein, suggesting that CDH3-10-807 peptide and KIF20A-10-66 peptide are naturally presented on HLA-A*2402 molecule of human cancer cells. Our results demonstrated that CDH3-10-807 peptide and KIF20A-10-66 peptide are novel HLA-A24-restricted tumor-associated antigens and would be applicable for CTL-inducing cancer therapies.

1. Introduction

After identification of the melanoma antigen gene (MAGE) family as a tumor-associated antigen (TAA), a number of TAAs have been revealed by means of various approaches including SEREX and cDNA library screening [1–6]. Some TAAs, such as MAGE, gp100, and MUC1, have been applied to treat various cancers in clinical trials [7–9], and vaccine-based therapy is now considered as a promising approach to fight against various cancers [10–13].

We have identified dozens of genes specifically expressed in cancer cells by genome-wide expression profile analysis for cDNA microarray consisting of more than 30,000 cDNAs and expressed sequence tags (ESTs) [14]. Among them, two genes, Cadherin 3, type 1, P-cadherin (CDH3) and kinesin family member 20A (KIF20A), were found to be upregulated in pancreatic cancers [15, 16]. CDH3 is one of the classic cadherin family that plays a critical role in cell-cell adhesion and epithelial morphogenesis [17]. We reported that over-expression of CDH3 promoted the motility of cancer cells and blocking of CDH3 by anti-CDH3 antibody inhibited the migration of CDH3-expressing cells [15]. KIF20A is a member of the kinesin family, which is characterized to be a motor protein in cancer cells [18], and northern analysis indicated no expression of KIF20A among examined 23 normal tissues except testis. Furthermore, knock down of KIF20A expression with small interfering RNA suppressed the proliferation of pancreatic ductal adenocarcinoma cells [16].

Thus, both CDH3 and KIF20A would play oncogenic functions in pancreatic cancer cells and are attractive target molecules for cancer therapies including immunotherapy.

We here identified CDH3- and KIF20A-derived novel HLA-A*2402-restricted epitope peptides that can induce peptide-specific cytotoxic T lymphocyte (CTL), suggesting that these epitope peptide would be applicable to peptide-based cancer vaccine therapies for HLA-A*2402 positive pancreatic cancer patients.

2. Materials and Methods

2.1. Peptides. CDH3 and KIF20A-derived 9-mer and 10-mer peptides that have high binding affinity (binding score > 10) to HLA-A*2402 were predicted by the binding prediction software "BIMAS" (http://www-bimas.cit.nih.gov/molbio/hla_bind/) and were synthesized by Sigma-Aldrich Japan KK (Ishikari, Japan) according to a standard solid-phase synthesis method and purified by reversed-phase high-performance liquid chromatography (HPLC). HIV-A24 epitope peptide (RYLRDQQLL) [19] was also synthesized as a negative control. The purity (>90%) and the identity of the peptides were confirmed by analytical HPLC and mass spectrometry analysis, respectively. Peptides were dissolved in dimethylsulfoxide at 20 mg/mL and stored at −80°C.

2.2. Cell Lines. CDH3- and KIF20A- negative Human B-lymphoblastoid cell line TISI (HLA-A*2402) was purchased from the IHWG Cell and Gene Bank (Seattle, WA). Monkey kidney cell line COS7, human B-lymphoblastoid cell line Jiyoye (HLA-A32), human B-lymphoblastoid cell line EB-3 (HLA-A3/Aw32), and CDH3-expressing human lung cancer cell line H358 (HLA-A3) were purchased from American Type Culture Collection (Manassas, VA). CDH3-expressing human pancreatic cancer cell line PK-45P (HLA-A24/A33) and KIF20A-expressing human pancreatic cancer cell line PK-59 (HLA-A31/A33) were provided by Cell Resource Center for Biomedical Research, Tohoku University (Sendai, Japan). KIF20A-expressing human stomach cancer cell line MKN-45 (HLA-A24) and MiaPaCa-2 cells (HLA-A24) were purchased from Health Science Research Resources Bank (Osaka, Japan). TISI, Jiyoye, EB-3, H358, PK-45P, PK-59, and MKN-45 were maintained in RPMI1640 media (Invitrogen, Carlsbad, CA), COS7 were maintained in DMEM media (Invitrogen), and MiaPaCa-2 cells were maintained in EMEM media (Invitrogen). Each medium was supplemented with 10% fetal bovine serum (GEMINI Bio-Products, West Sacramento, CA) and 1% antibiotic solution (Sigma-Aldrich, ST. Louis, MO). The expression of CDH3 and KIF20A protein was confirmed by Western blotting using anti-CDH3 antibody (BD Transduction Labs., BD Biosciences, San Jose, CA) or anti-KIF20A antibody (Bethyl Laboratories, Montgomery, TX).

2.3. In Vitro Induction of Peptide-Specific CTL. To examine the ability to induce peptide-specific CTL, purified $CD8^+$ T cells were cocultured with autologous monocyte-derived mature dendritic cells (DCs) pulsed with peptide. Both $CD8^+$ T cells and DCs were prepared from peripheral blood mononuclear cells (PBMCs) of same HLA-A*2402-positive healthy volunteers. Briefly, PBMCs were isolated by Ficoll-Paque solution (GE Healthcare, Uppsala, Sweden), then cells were cultured in AIM-V medium (Invitrogen) containing 2% heat-inactivated autologous serum (AS). After the over night incubation, nonadherent cells were washed out, then 1000 U/mL of granulocyte-macrophage colony-stimulating factor (GM-CSF; R&D Systems, Minneapolis, MN) and 1000 U/mL of interleukin (IL)-4 (R&D Systems) were added in the culture to induce monocyte-derived DCs. To mature DCs, 0.1 KE/mL of OK-432 (Chugai Pharmaceutical Co., Tokyo, Japan) was added in the culture on day 5. Seven days later, DCs were pulsed with 20 μg/mL of synthesized peptide in AIM-V medium containing 3 μg/mL of β2-microglobulin (Sigma-Aldrich) at 37°C for 3 h [20] and incubated in the media containing 30 μg/mL of Mitomycin C (MMC) (Kyowa Hakko Kirin Co. Ltd., Tokyo, Japan) for 30 min. Following washing out residual peptide and MMC, cells were used as antigen-presenting cells to induce peptide-specific CTL. Generated monocyte-derived mature DCs expressed CD80, CD83, CD86, and HLA class II on their cell surface (data not shown). Autologous $CD8^+$ T cells were prepared from PBMCs derived from the same HLA-A*2402-positive donor by positive selection with Dynal CD8 positive isolation kit (Invitrogen) according to the manufacturer's instructions. 1.5×10^4 of peptide-pulsed DCs and 3×10^5 of $CD8^+$ T cells were cocultured in 0.5 mL of AIM-V medium supplemented with 10 ng/mL of IL-7 (R&D Systems) and 2% AS on 48-well plates (Corning Inc., Corning, CA). IL-2 (CHIRON, Emeryville, CA) was added to the culture at 20 IU/mL 3 days after coculture, and peptide-pulsed DCs were additionally supplied into the culture on days 7 and 14. Eight wells were prepared for CTL induction by every peptide in a single experiment. On day 21, interferon- (IFN-) γ production was examined by IFN-γ enzyme-linked immunospot (ELISPOT) assay under the stimulation with peptide-pulsed TISI cells.

2.4. IFN-γ Enzyme-Linked Immunospot (ELISPOT) Assay. T cell response to epitope peptide was measured by ELISPOT assay using IFN-γ ELISPOT kit and AEC substrate set (BD Pharmingen, San Diego, CA) according to the manufacturer's instruction. Briefly, TISI cells were pulsed with 20 μg/mL of respective peptide at 37°C for 20 h, and the residual peptide that did not bind to TISI cells was washed out to prepare peptide-pulsed TISI cells as the stimulator cells. 200 μL of cell culture suspension were distributed to two wells (100 μL each) on Multiscreen-IP 96-well plate (Millipore, Bedford, MA) following removing 500 μL of supernatant from each well from culture of "*in vitro* induction of peptide-specific CTL." Cells were co-incubated with peptide-pulsed TISI cells (1×10^4 cells/well) at 37°C for 20 h. The plates were analyzed by the automated ELISPOT reader, ImmunoSPOT S4 (Cellular Technology Ltd, Cleveland, OH) and ImmunoSpot Professional Software Version 5.0 (Cellular Technology Ltd). TISI cells pulsed with HIV-A24 epitope peptide (RYLRQQLLGI) were used as control. When the spot number in the peptide-stimulating

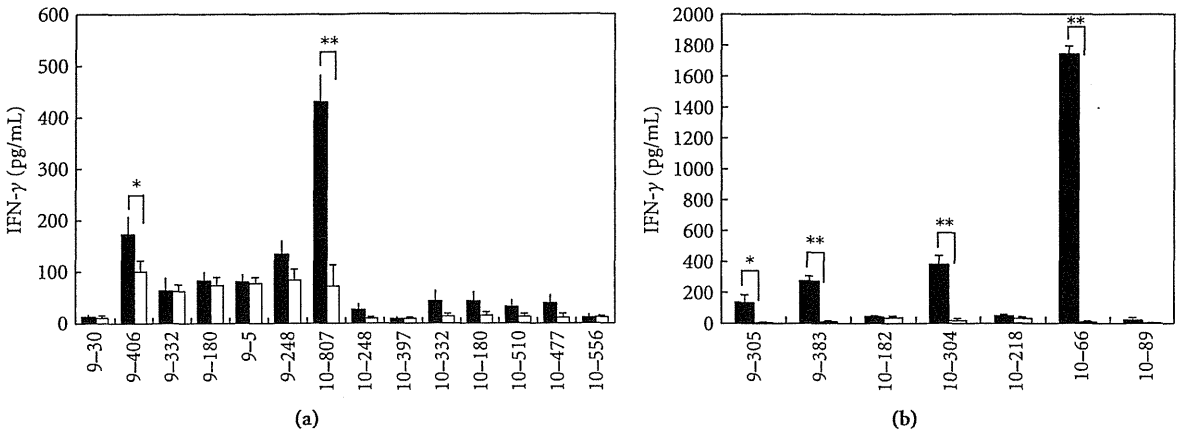

FIGURE 1: IFN-γ production from CTLs responding to CDH3- or KIF20A-derived peptides. IFN-γ production by CTLs induced with CDH3-derived peptides (a) or KIF20A-derived peptides (b) responding to respective peptide-pulsed HLA-A*2402 positive TISI cells. CTLs were expanded and harvested following "*in vitro* induction of peptide-specific CTL," and IFN-γ production was examined by IFN-γ ELISA. "Closed bar" indicates the mean IFN-γ production responding to TISI cells pulsed with indicated peptide, and "open bar" indicates the mean IFN-γ production responding to TISI cells pulsed with HIV-A24 peptide (negative control). All experiments were performed triplicate. Similar results were obtained in three to five independent experiments. $*P < 0.05$, $**P < 0.01$.

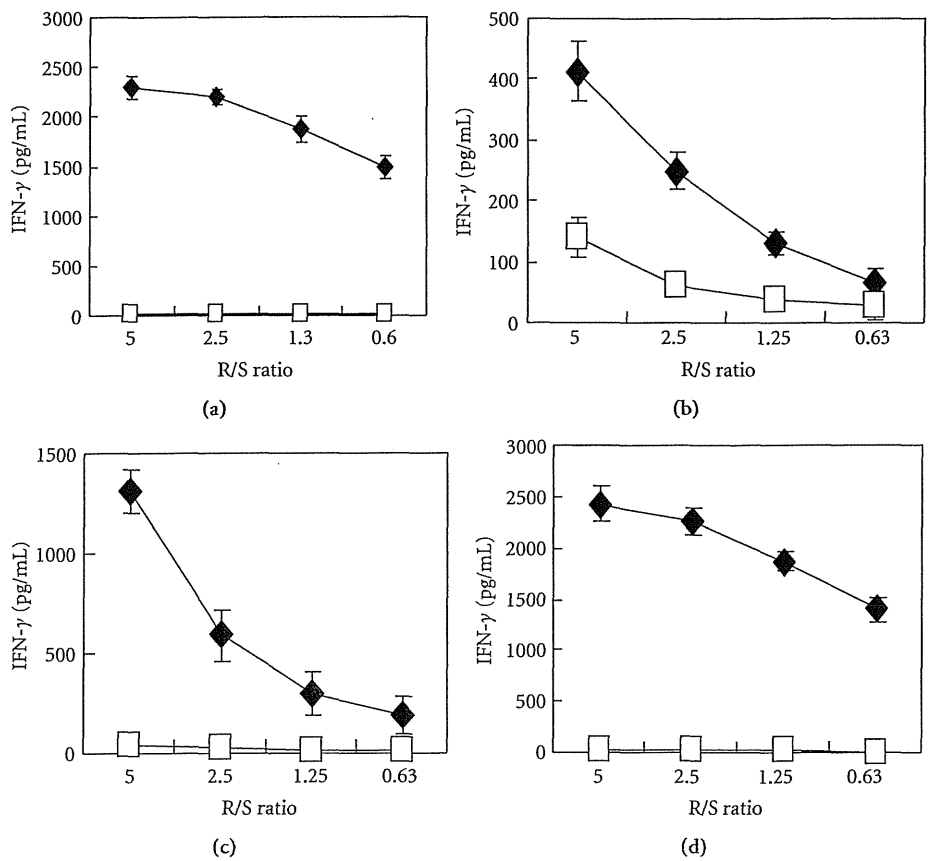

FIGURE 2: Peptide-specific IFN-γ production by CTL clones. IFN-γ production by CDH3-10-807 peptide-specific CTL clone (a), KIF20A-9-305 peptide-specific CTL clone (b), KIF20A-10-304 peptide-specific CTL clone (c), and KIF20A-10-66 peptide-specific CTL clone (d), when stimulated with TISI cell pulsed with corresponding peptide (closed diamond) or HIV-A24 peptide (open square). CTL clones produced significant amount of IFN-γ responding to corresponding peptide. IFN-γ ELISA was performed triplicate. R/S ratio, responder cell (CTL clone)/stimulator cell (TISI cell) ratio.

Table 1: Candidates of epitope peptide derived from CDH3 and KIF20A.

CDH3				KIF20A			
Start position	Amino acid sequence (mer)	Binding score	CTL induction	Start position	Amino acid sequence (mer)	Binding score	CTL induction
513	IYEVMVLAM (9)	37.5	–	308	IYNELLYDL (9)	432	–
667	LFLLLVLLL (9)	36	–	621	MYEEKLNIL (9)	432	–
30	VFREAEVTL (9)	24	+	67	VYLRVRPLL (9)	420	–
406	LYVEVTNEA (9)	16.6	+	499	KFSAIASQL (9)	56	–
332	KYEAHVPEN (9)	16.5	+	304	SFFEIYNEL (9)	44.352	–
180	KYELFGHAV (9)	15	+	187	IFNSLQGQL (9)	36	–
85	RSLKERNPL (9)	14.4	–	305	FFEIYNELL (9)	30	+
5	RGPLASLLL (9)	12	+	23	MFESTAADL (9)	30	–
652	KGGFILPVL (9)	11.2	–	256	SFDSGIAGL (9)	20	–
248	TYNGVVAYS (9)	10.5	+	298	RFSIWISFF (9)	20	–
65	LFSTDNDDF (9)	10	–	383	IFSIRILHL (9)	20	+
807	DYLNEWGSRF (10)	150	+	647	KIEELEALL (9)	17.28	–
248	TYNGVVAYSI (10)	105	+	625	KLNILKESL (9)	14.4	–
667	LFLLLVLLLL (10)	42	–	695	KLQQCKAEL (9)	13.2	–
397	DFEAKNQHTL (10)	30	+	726	FTIDVDKKL (9)	11.088	–
332	KYEAHVPENA (10)	21	+	688	QLQEVKAKL (9)	11.088	–
180	KYELFGHAVS (10)	15	+	308	IYNELLYDLL (10)	432	–
510	RNNIYEVMVL (10)	12	+	182	RSLALIFNSL (10)	24.192	+
5	RGPLASLLLL (10)	12	–	304	SFFEIYNELL (10)	24	+
477	RILRDPAGWL (10)	12	+	742	RLLRTELQKL (10)	15.84	–
556	CNQSPVRQVL (10)	10.1	+	739	KNIRLLRTEL (10)	15.84	–
				218	RQEEMKKLSL (10)	14.4	+
				70	RVRPLLPSEL (10)	12.672	–
				871	RILRSRRSPL (10)	12	–
				89	RIENVETLVL (10)	12	+
				364	KNQSFASTHL (10)	12	–
				66	KVYLRVRPLL (10)	11.2	+
				60	DSMEKVKVYL (10)	10.08	–

Start position indicated the number of amino acids from the N terminal of CDH3 and KIF20A.
Binding score was obtained using BIMAS program.
CTL induction was indicated as positive (+) or negative (–). Similar results were obtained 3–7 independent experiments using PBMC of 3–7 healthy volunteers.

well was more than 50 spots/well compared with that in the control well, we estimated that peptide-specific CTL were induced (positive) and subsequently expanded CTL from the positive well. Sensitivity of our ELISPOT assay was estimated as approximately average level by ELISPOT panel of Cancer Immunotherapy Consortium [CIC (http://www.cancerresearch.org/consortium/assay-panels/)].

2.5. CTL Expansion. Peptide-specific CTL obtained from CTL positive well of "*in vitro* induction of peptide-specific CTL" were expanded by the modified protocol based on the previously described methods [21–24]. Briefly, 5×10^5 of CTLs were cocultured with 5×10^6 of MMC-treated (30 μg/mL at 37°C for 30 min) EB-3 and Jiyoye cells in 25 mL of AIM-V containing 5% AS and 40 ng/mL of anti-CD3 mAb. The cultures were supplemented with IL-2 (final concentration: 120 IU/mL) 24 h later and fed with AIM-V medium containing 5% AS and IL-2 (30 IU/mL) on day 5, 8, and 11. On day 14, expanded T cells were harvested to examine specific response to epitope peptide by IFN-γ enzyme-linked immunosorbent assay (ELISA).

2.6. Establishment of Peptide-Specific CTL Clone. Peptide-specific CTL clones were established by limiting dilution method from the expanded CTLs specifically responding to epitope peptide. Briefly, T cells were diluted to 0.3, 1, and 3 cells/well in 96-well round-bottomed plates and cultured with 1×10^4 cells/well of MMC-treated EB-3 and Jiyoye cells in 150 μL of AIM-V containing 5% AS, 125 IU/mL of IL-2, and 30 ng/mL of anti-CD3 mAb. The culture was supplemented with IL-2 to the final concentration of 125 IU/mL on day 10. On day 14, IFN-γ production from peptide-specific CTL clones was examined by IFN-γ ELISA. Some peptide-specific CTL clones were expanded as described above.

2.7. IFN-γ ELISA. In some experiments, established CTLs were co-incubated with 1×10^4 cells of respective peptide-pulsed TISI cells or 5×10^4 cells of COS7 cells in 200 μL of AIM-V/5% AS media on 96-well round bottom plate (Corning Inc.). After 24 h incubation, cell free supernatants were harvested and IFN-γ production was examined by human

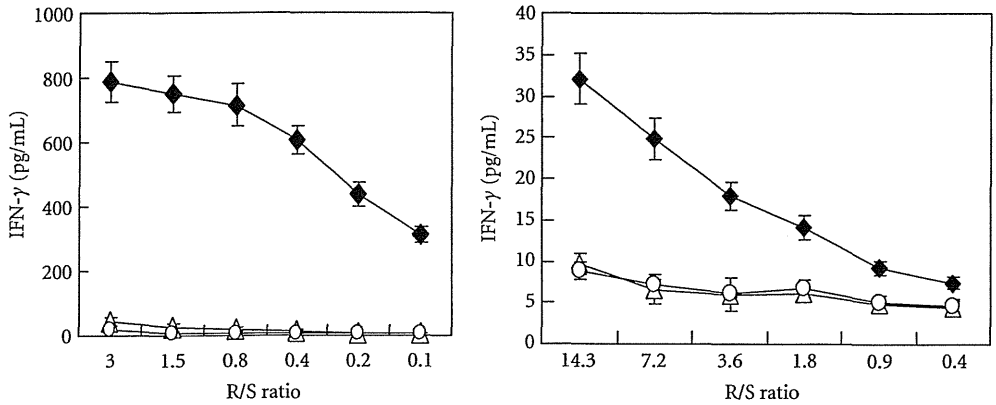

FIGURE 3: IFN-γ production by CTL clones responding to COS7 cells that expressing HLA-A*2402 and respective oncogene. (a) IFN-γ production by CDH3-10-807 peptide-specific CTL clone when exposed with COS7 cells expressing both HLA-A*2402 and CDH3 (closed diamond), HLA-A*2402 (open triangle), or CDH3 (open circle). (b) IFN-γ production by KIF20A-10-66 peptide-specific CTL clone when exposed with COS7 cells expressing HLA-A*2402 and KIF20A (closed diamond), HLA-A*2402 (open triangle), or KIF20A (open circle). Both CTL clones significantly produced IFN-γ responding to COS7 cells expressing HLA-A*2402 and corresponding gene. Similar results were obtained in three independent experiments. Independently induced other CTL clones also produced significant amount of IFN-γ when exposed with COS7 cell expressing both HLA-A*2402 and respective gene (data not shown). R/S ratio, responder cell (CTL clone)/stimulator cell (COS7 cell) ratio.

IFN-γ-specific ELISA kit (BD Pharmingen) according to the manufacturer's instructions.

2.8. Cytotoxicity Assay. Specific cytotoxic activity of induced CTL clones was tested by a 4 h ^{51}Cr release assay as previously described [25]. Data are represented as the mean ± SD of triplicate samples.

2.9. Transfection of HLA-A24 and/or Oncogene (CDH3 or KIF20A). HLA-A*2402 coding region was obtained from TISI cells. The cDNA encoding an open reading frame of HLA-A*2402 gene with FLAG tag or oncogene (CDH3 or KIF20A) coding region with the Myc tag sequence was amplified with PCR and cloned into pcDNA3.1 vector (Invitrogen). COS7 cells transiently expressing HLA-A*2402 and/or oncogene were prepared by the transfection of the vectors encoding respective genes using lipofectamine 2000 (Invitrogen) according to the manufacturer's instruction. The expression of HLA-A*2402 and oncogene-derived protein was confirmed by Western blotting using anti-Myc (Upstate Biotechnology, Lake Placid, NY) or anti-FLAG antibody (Sigma-Aldrich). Two days after transfection, the transfected cells were harvested with versene (Invitrogen) and used to stimulate peptide-specific CTL clones. IFN-γ production by CTLs was examined by IFN-γ-specific ELISA.

2.10. Flow Cytometry. Expression of peptide-specific T cell receptor (TCR) was examined on FACS-CantoII (Becton Dickinson, San Jose, CA) using peptide-HLA-A*2402 dextramer-PE (Immudex, Copenhagen, Denmark) (CDH3-10-807/MHC-dextramer-PE and KIF20A-10-66/MHC-dextramer-PE) according to the manufacturer's instructions. HIV-A24 epitope peptide (RYLRDQQLL)/MHC-dextramer was used as negative control. Briefly, expanded CTL lines were incubated with peptide-HLA-A*2402 dextramer-PE for 10 minutes at room temperature, then treated with FITC-conjugated anti-human CD8 mAb, APC-conjugated anti-human CD3 mAb, PE-Cy7-conjugated anti-human CD4 mAb, and 7-AAD (BD Pharmingen) at 4°C for 20 minutes.

3. Results

*3.1. Induction of CTL Responding to CDH3- or KIF20A-Derived Peptide Restricted with HLA-A*2402.* Based on the analysis with the binding prediction software "BIMAS," we synthesized 21 CDH3-derived epitope-peptides and 28 KIF20A-derived epitope-peptides that were expected to have high affinity to HLA-A*2402 molecule and activate CTLs (Table 1).

HLA-A*2402-positive CD8$^+$ T cells were cocultured with autologous DCs pulsed with respective peptide, and then peptide-specific IFN-γ production was analyzed by ELISPOT. Fourteen peptides derived from CDH3 and 7 peptides derived from KIF20A were able to induce peptide-specific CTLs producing IFN-γ (Table 1). Amongst these peptides, we successfully obtained CTLs that specifically produced significant amount of IFN-γ after CTL expansion when CDH3-9-406, CDH3-10-807, KIF20A-9-305, KIF20A-9-383, KIF20A-10-304, and KIF20A-10-66 peptide were pulsed (Figures 1(a) and 1(b)).

3.2. Establishment of CDH3- or KIF20A-Derived Peptide-Specific CTL Clones. Subsequently, we attempted to establish CTL clones by a limiting dilution. CDH3-10-807-, KIF20A-9-305-, KIF20A-10-304-, or KIF20A-10-66-specific CTL clones were established and produced a potent amount of

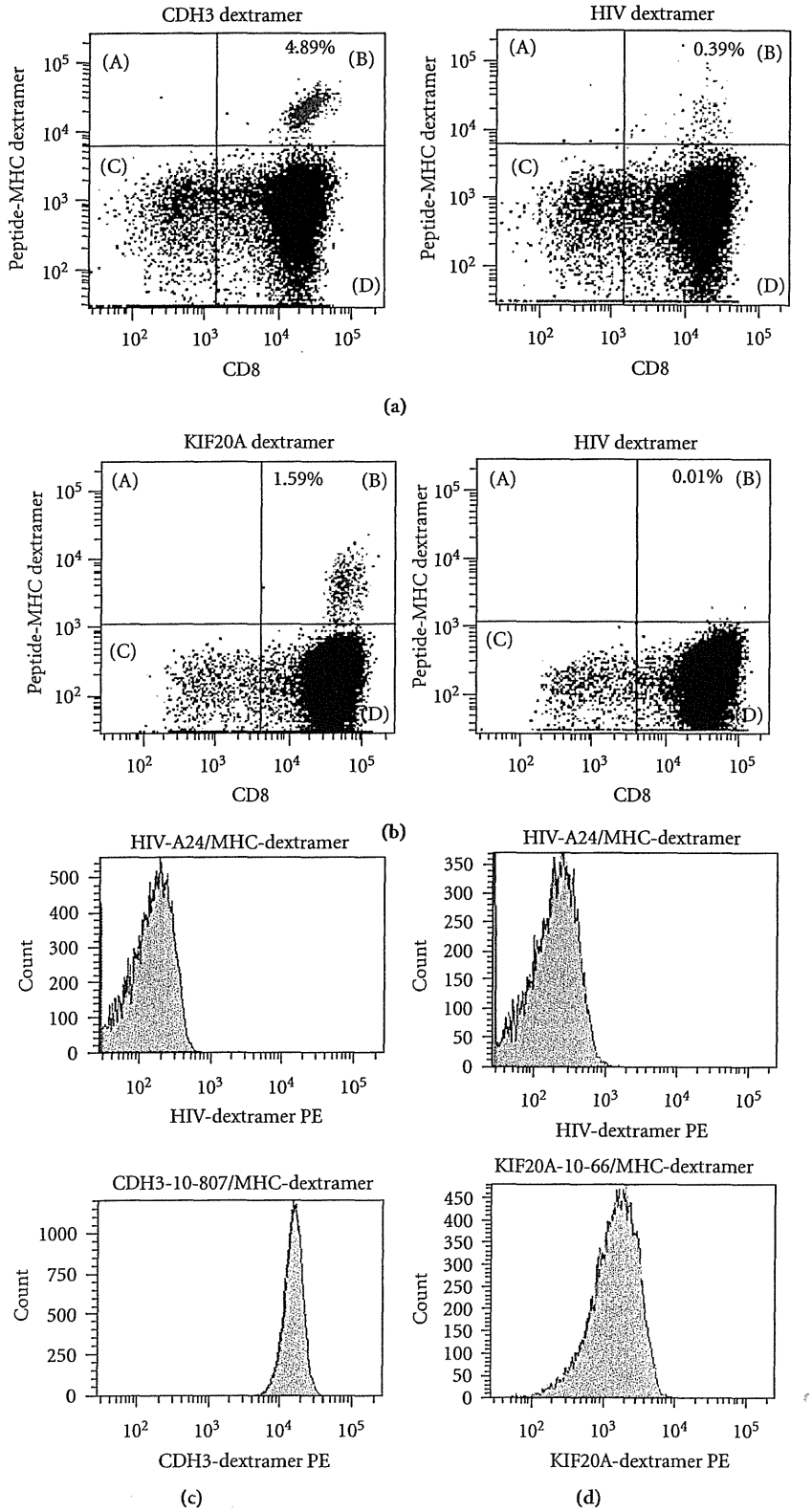

FIGURE 4: Peptide-specific TCR expression on CTL clones. (a) CDH3-10-807/HLA-A*2402-specific TCR expressing cells in expanded CTLs following "*in vitro* induction of peptide-specific CTL." (b) KIF20A-10-66/HLA-A*2402-specific TCR expressing cells in expanded CTLs following "*in vitro* induction of peptide-specific CTL." Results staining with anti-human CD8 mAb and CDH3-10-807/MHC-dextramer-PE or KIF20A-10-66/MHC-dextramer-PE are presented following gating on CD3-positive cells (left panels). Results staining with anti-human CD8 mAb and HIV-A24/MHC-dextramer-PE are presented as negative control following gating on CD3 positive cells (right panels). (c) CDH3-10-807/HLA-A*2402-specific TCR expression on CDH3-10-807-specific CTL clone. (d) KIF20A-10-66/HLA-A*2402-specific TCR expression on KIF20A-10-66-specific CTL clone. Staining with HIV-A24/MHC-dextramer-PE was used as negative control. CTL clones were $CD3^+$ and $CD8^+$ as expected (data not shown). Similar results were obtained in independent all experiments to examine CTL induction.